
A SURVEY OF DEEP CAUSAL MODELS

Zongyu Li, Zhenfeng Zhu*, Zhenyu Guo, Shuai Zheng, Yao Zhao

School of Computer and Information Technology, Beijing Jiaotong University, Beijing, China
Beijing Key Laboratory of Advanced Information Science and Network Technology,
Beijing, China

zongyuli, zhfhzhu, zhyguo, zs1997, yzhao@bjtu.edu.cn

ABSTRACT

The concept of causality plays a significant role in human cognition. In the past few decades, causal inference has been well developed in many fields, such as computer science, medicine, economics, and other industrial applications. With the advancement of deep learning, it has been increasingly applied in causal inference against counterfactual data. Typically, deep causal models map the characteristics of covariates to a representation space and then design various objective functions to estimate counterfactual data unbiasedly. Different from the existing surveys on causal models in machine learning, this paper mainly focuses on the overview of the deep causal models, and its core contributions are as follows: 1) we summarize the popularly adopted relevant metrics under multiple treatments and continuous-dose treatment; 2) we cast insight on a comprehensive overview of deep causal models from both timeline of development and method classification perspectives; 3) we also endeavor to present a detailed categorization and analysis on relevant datasets, source codes and experiments.

1 Introduction

In general, causality refers to the connection between an effect and the cause of it. Causes and effects of this phenomenon are difficult to define, and we are often only aware of them intuitively[1]. Causal inference is a process of drawing a conclusion about a causal connection based on the circumstances surrounding the occurrence of the effect and has a variety of applications in real-world scenarios[2]. For example, estimating causal effects of observational data in advertising[3, 4, 5, 6, 7, 8, 9], developing recommender systems that are highly correlated with causal treatment effect estimates[10, 11, 12, 13, 14, 15, 16], learning optimal treatment rules for patients in medicine[17, 18, 19], estimation of ITE in reinforcement learning[20, 9, 21, 22, 23, 24, 25, 26, 27], causal inference tasks in natural language processing[28, 29, 30, 31, 32, 33], emerging computer vision and language interaction tasks[34, 35, 36, 37, 38], education[39], policy decisions[40, 41, 42, 43, 44], and improved machine learning[45], etc.

Deep learning largely contributes to the development of artificial intelligence when applied to big data[46, 47, 48, 49]. In comparison with traditional machine learning, deep learning models are more computationally efficient, more accurate, and hold good performance in various fields. However, many deep learning models are black boxes with poor interpretability since they are more interested in correlations than causality as inputs and outputs[50, 51, 52]. In recent years, deep learning models have been widely used for mining data for causality rather than correlation[40, 42]. Thus, deep causal models have become a core method for estimating treatment effects based on unbiased estimates[19, 43, 44, 53]. At present, many works in the field of causal inference utilize deep causal models to select reasonable treatment options[54, 55, 56, 57].

With the emergence of big data, all trend variables are tended to be correlated[58], so discovering the latent causal relationships is becoming one of challenging problems[59, 60, 61]. In terms of statistical theory, it is the most effective way to conduct **randomized controlled trials(RCT)**[62] to infer causality. In other words, the sample is randomly assigned to a treatment or control group. Despite this, real-world RCT data are sparse and have several serious deficiencies. The studies involving RCTs require a large number of samples with little variation in characteristics,

*Corresponding author

| Surveys | Highlights |
|--|--|
| The Development of Causal Reasoning[79] | The origin and development of causal reasoning |
| Causality for Machine Learning[80] | The connection between graphical causal inference and machine learning |
| Causal Inference[81] | Machine Learning Interpretability for Counterfactual Causal Reasoning |
| Toward Causal Representation Learning[82] | Exploring causal variables in data through causal representation learning |
| Causal Machine Learning for Healthcare and Precision Medicine[83] | Causal Machine Learning in clinical decision support systems |
| A Survey of Learning Causality with Data: Problems and Methods[1] | The relationship between causal learning and machine learning in big data |
| A Survey on Causal Inference[2] | Causal effect estimation of observational data in the potential outcomes framework |
| A Review and Roadmap of Deep Learning Causal Discovery in Different Variable Paradigms[84] | An improved exploration of causal discovery from the perspective of deep learning and variable paradigms |
| Causal Machine Learning: A Survey and Open Problems[86] | Five types of causal machine learning problems under structural causal models |
| Causal Inference in Recommender Systems: A Survey and Future Directions[85] | Optimize the recommendation system by extracting causality through causal reasoning |
| A Survey of Deep Causal Models | In-depth causal inference model from perspective of deep network development |

Table 1: **Highlights of existing surveys on causal learning**

which is difficult to interpret and will further involve some ethical issues inevitably. As a matter of fact, it is also not wise to select subjects to try a drug or vaccine[63, 64] in the process of drug development. Therefore, causal effects are usually measured directly using observational data. A central question for obtaining counterfactual results is how to deal with observational data[65]. When observational data are analyzed, treatments are not randomly assigned and the performance of samples after treatment is significantly different from the one of ordinary samples[40, 42]. Unfortunately, we can’t observe alternative outcomes in theory since the counterfactual results[66] are not available to be observed. For a long time, mainstream research has mainly explored the use of the potential outcome framework as a means of addressing the problem of causal inference from observational data[67]. The potential outcome framework is also known as the Rubin Causal Model[68]. In essence, causal inference is closely connected to deep learning since it is conceptualized using Rubin Causal Model. In order to enhance the accuracy and unbiasedness of estimates, there are some works that attempt to combine deep networks and causal models. Just to illustrate several of them, e.g., the methods considering representations of distribution balance[40, 42, 43], exploiting the effects of covariates confounding learning[53, 69, 70, 71], the methods based on generative adversarial networks[44, 72, 73, 74], and so forth[57, 33, 75]. Due to the simultaneous development of deep learning and causal inference, the problem of deep causal models has become more open and diverse[76, 77, 78].

In recent years, various perspectives have been discussed regarding causal inference[79, 1, 80, 81, 82, 83, 84, 85, 2, 86]. In Table 1, we list some of existing representative surveys and their highlight points. An in-depth analysis of the origin and development of causal inference was provided in review[79], as well as the implications of causal learning for the development of causal inference. Immediately after that, due to the rapid development of the field of machine learning, a detailed discussion of the relevance of graphical causal inference to machine learning was presented in survey[80]. In addition, an overview of traditional and cutting-edge causal inference methods and the comparison between machine learning and causal learning can be found in survey[1]. As one of hot focuses in recent years, the studies on the interpretability of machine learning have received great attention. An analytical summary of relevant interpretable artificial intelligence algorithms was elaborated in [81] by combining causal inference with machine learning. Moreover, with the flourishing of causal representation learning, review[82] takes this new perspective to uncover high-level causal variables from low-level observations, strengthening the link between machine learning and causal inference. In survey[86], the structural causal model of counterfactual intervention was comprehensively explained and summarized, and five classes of problems under causal machine learning are systematically analyzed and compared. Furthermore, in review[83], the authors discussed the way in which the latest progress of machine learning is applied to causal inference, and provides a in-depth interpretation of how causal machine learning can contribute to the advancement in healthcare and precision medicine. As argued in review[84], causal discovery methods can be improved and sorted out based on deep learning, and can also be considered and explored from a variable paradigm perspective. Causal inference in recommender systems is the focus of survey[85], which explains how causal inference can be used to extract causal relationships to enhance recommender systems. The potential outcome framework in statistics has long served as a bridge between causal inference and deep learning. As a starting point, review[2] analyzes and compares different classes of traditional statistical algorithms and machine learning that satisfy these assumptions. Given the rapid development of deep learning, the existing literature fails to take deep causal models into full account when studying generalization problems. Therefore, from the perspective of deep neural network, we summarize the deep causal model in terms of temporal progress and classification. Particularly, this survey provides a comprehensive review and analysis of deep causal models in recent years, which makes three core contributions: 1) we summarize the popularly adopted relevant metrics under multiple treatments and continuous-dose treatment; 2) we cast insight on a comprehensive overview of deep causal models from both temporal development and method classification perspectives; 3) we also try to present a detailed categorization and analysis on relevant datasets, source codes and experiments.

The rest of the paper is outlined as follows. In Section 2, some relevant definitions and assumptions of causal inference are inducted. Then, in Section 3, we present the classical examples and metrics, including binary treatment, multiple

treatment, and continuous dose treatment. The deep causal model is comprehensively elaborated in Section 4. Next, we categorize the deep causal modeling methods into five groups in Section 5, including representation learning for distribution balancing, covariates confounding learning, methods based on generative adversarial networks, time series causal estimation problem, and methods based on multi-treatment and continuous-dose treatment models. After that, the relevant experimental guidelines are listed in Section 6. Finally, we conclude this article in Section 7.

2 Preliminaries

In this section, we present the background knowledge of causal inference, including task descriptions, mathematical concepts, and pertinent assumptions.

Basically, the aim of causal inference is to estimate the change in outcome that will occur if a different treatment are implemented[2]. Imagine that there are several treatment plans A, B, C, and so on, all of which have different cure rates, and the change in the cure rate is the result of the treatment scheme. Realistically, we can't apply different treatment regimens to the same group at the same time. As opposed to RCT, the main problem to be solved in observational research is the lack of counterfactual data. In other words, the challenge we face is how to find the most effective treatment plan based on past experimental diagnosis and medical history of the patient.

Because of the widespread accumulating of data in fields such as health care[87, 88, 89], sociology science[90, 91, 92, 93], digital marketing[94, 4, 5], and machine learning[95, 96, 9, 97, 98], observational studies are becoming increasingly important. To cater to this trend, deep causal models neural networks have also been widely used to make counterfactual estimates based on observational data, which can further aid to make optimal treatment decisions in various fields.

2.1 Definitions

Here, to make the survey self-consistent, we first give some basic definitions under the potential outcome framework[68]. In particular, causality is defined as the result of a treatment scheme applied to a sample, which can either be a specific behavior, a specific method, or some specific treatment scheme. The followings are the concepts related to causal effect estimation, which are benchmarked against the relevant basic definitions in the survey[2].

Definition 1 *Treatment Effect Estimation(Causal Effect Estimation):* Estimate the change in outcome of a given sample receiving an intervention.

Treatment effect estimation and lift modelling have the same goal, the difference is: the lift model is on random experimental data, treatment effect estimates usually need to adhere to the necessary assumptions, applied to experimental and observational data.

Definition 2 *Sample:* A sample is also referred to as a unit, that is, an atomic study object.

Typical samples include a person, a patient, an object, a collection of objects or people at a particular time, a classroom, or a marketplace[99]. A sample of the whole population is equivalent to a unit in the dataset.

Definition 3 *Treatment:* A treatment refers to a scheme or action applied to a sample.

As a medical term, a drug scheme is a treatment. For binary treatments, $T = 1$ is the *treated group*, and $T = 0$ is the *control group*. Multiple treatments can be indicated by the $T \in \{0, 1, 2, \dots, T_N\}$, where $N + 1$ denotes the total number of treatments.

Definition 4 *Observed outcome:* An observational outcome, also known as a factual outcome, is a measure of how the sample's outcomes applied to the treatment.

In the case of a specific treatment, observed outcomes can be displayed in Y^F , where $Y^F = Y(T = T_i)$. A donation of in the amount of Y_{T_i} is made as *potential outcome*[99].

Definition 5 *Counterfactual outcome:* A counterfactual outcome is the outcome that differ from a factual outcome.

With binary treatments, counterfactual outcome is denoted as Y^{CF} , and $Y^{CF} = Y(T = 1 - T_i)$. Assuming multiple treatments, let $Y^{CF}(T = T'_i)$ donate the counterfactual result of treatment T'_i .

Definition 6 *Dose:* A dose refers to the amount of drug taken continuously during a particular course of treatment.

In general, there are many medical treatments involving continuous dose parameters, such as vasopressors[100]. A set of continuous dose regimens can be denoted as D_T , the treatment-specific factual doses can be denoted as D^F , and $D^F = D(T = T_i)$. Simultaneously, counterfactual dose can be denoted as $D^{CF}(T = T'_i)$.

Definition 7 *Dose-response curve:* A dose-response curve indicates the effect of the samples' response over time after receiving different doses of the intervention.

A better fit to the dose-response curve could make the model more robust and expressive in continuous dose treatments. The actual and counterfactual outcomes on the dose-response curves can be expressed as the sets $Y^F(D^F, T_i)$ and $Y^{CF}(D^{CF}, T'_i)$.

Definition 8 *Covariates:* Covariates are variables that are unaffected by treatment choice.

Generally, covariates in the healthcare setting refer to the patient's demographic, medical history, experimental data, etc., usually denoted by X . Covariates can be separated into confounding and non-confounding variables, specifically divided into three categories[69]: instrumental factor I , which only affect treatment T ; confounding factor C , which contribute to both treatment T and outcome Y ; and adjustment factor A , which only determine outcome Y .

2.2 Assumptions

After understanding the basic definition of causal inference, the following three assumptions, which are derived from papers[2, 81], are commonly required to achieve the estimation of causal treatment effects.

Assumption 1 *Stable Sample Treatment Value (SSTV):* One sample's response to treatment is independent of the assignment of other samples.

Based on this assumption, there is no interaction between samples, and there is only one version of each treatment option. SSTV assumption can be expressed as $P(Y_i|T_i, T'_i, X_i) = P(Y_i|T_i, X_i)$.

Assumption 2 *Ignorability:* Given the covariate X , the treatment distribution T is independent of the potential outcomes.

In the assumption of ignorability, there should be no unobserved confounding factors. $T \perp\!\!\!\perp Y(T = T_i), Y(T = T'_i)|X$ needs to be satisfied.

Assumption 3 *Overlap:* When given the observed variables, each sample has nonzero probability to receive either treatment status.

In order to estimate the counterfactual treatment effect, it must be assumed that each sample can implement any treatment option, otherwise the overlap assumption will not be valid. That is, $0 < P(T = T_i|X = x) < 1$ and $0 < P(T = T'_i|X = x) < 1$.

3 Treatments and Metrics

Deep causal models utilize different metrics to address different practical issues. For instances, in medicine[40, 42], health care[101, 75], markets[102], job searches[43, 44], social economy[73, 56], and advertising[41, 77], it may come to binary treatment problems, multi-treatment problems, or continuous dose treatment problems.

This section provides an analysis and description of the different performance metrics adopted for different classical application scenarios. In addition to the basic metrics in survey[2], we expand the evaluation from binary to multiple and continuous dose cases.

3.1 Binary treatment

Treatment refers to the action of a sample or a subject. In the medical field, a medication regimen for a patient is a treatment. When there are only two treatment options, the group of units applied with treatment $T = 1$ is the treated group, and the group of units with $T = 0$ is the control group, which can be referred to as the binary treatment[2].

In the binary treatment situation, the most basic and common performance metric is **Average Treatment Effect(ATE)**, which is defined as[103]:

$$ATE = \mathbb{E}[Y(T = 1) - Y(T = 0)], \quad (1)$$

where $Y(T = 1)$ and $Y(T = 0)$ indicate the results of the treatment and control groups in the population. This metric is commonly used to estimate causal effects for the well-known dataset IHDP[104]. Differentiate between treatment and control groups by whether intensive high-quality child care is applied, and the outcome is a score on the cognitive test for the infant.

In a sample set, the treatment effect is called the **Conditional Average Treatment Effect (CATE)** that is given as follows[2]:

$$\text{CATE} = \mathbb{E}[Y(T = 1)|X = n] - \mathbb{E}[Y(T = 0)|X = n], \quad (2)$$

where $Y(T = 1)|X = n$ and $Y(T = 0)|X = n$ represent the results under the sample set for the treatment and control groups with $X = n$, respectively. Since different treatments have different effects on different example sets, CATE is also known as heterogeneous treatment effect.

The treatment effect at the individual level is called **Individual Treatment Effect (ITE)**, which is defined as[2]:

$$\text{ITE}_n = Y_n(T = 1) - Y_n(T = 0), \quad (3)$$

where $Y_n(T = 1)$ and $Y_n(T = 0)$ represent the results of the sample in the treatment and control groups.

It is also helpful to keep in mind another evaluation metric, which is called **Precision in Estimation of Heterogeneous (PEHE)**. Regardless of fact or counterfactual outcomes, PEHE, as defined below[44], can perform unbiased estimates:

$$\text{PEHE} = \sqrt{\frac{1}{N} \sum_{n=1}^N (Y_1^F(n) - Y_0^F(n) - (Y_1^{CF}(n) - Y_0^{CF}(n)))^2} \quad (4)$$

where $Y_1^F(n)$, $Y_0^F(n)$ and $Y_1^{CF}(n)$, $Y_0^{CF}(n)$ respectively indicate unbiased estimates of the facts and the counterfactuals for the treatment and control groups. The Twins[53] dataset is typical of the application of this metric, and the result is a one-year mortality rate for children.

For the treated group, the treatment effect is referred to as the **Average Treatment effect on the Treated group (ATT)**, which is defined as[2]:

$$\text{ATT} = \mathbb{E}[Y(T = 1)|T = 1] - \mathbb{E}[Y(T = 0)|T = 1], \quad (5)$$

where $Y(T = 1)|T = 1$ and $Y(T = 0)|T = 1$ correspond to potential treated and control outcome of the treated group respectively. This metric is available for the jobs dataset[91], treatment group take part in vocational training, while the control group are not and the outcome is employment status.

Since only factual data is available for Jobs dataset, the testing set is from RCT. Therefore, heterogeneity effect indicators only can be described by **Policy Risk** ($\mathcal{R}_{pol}(\pi)$), which is defined as[42]:

$$R_{pol}(\pi) = \frac{1}{N} \sum_{n=1}^N \left[1 - \left(\sum_{i=1}^K \left[\frac{1}{|\Pi_i \cap T_i \cap E|} \sum_{X(n) \in \Pi_i \cap T_i \cap E} Y_i^F(n) \times \frac{|\Pi_i \cap E|}{|E|} \right] \right) \right] \quad (6)$$

where $\Pi_i = \{X(n) : i = \arg \max Y^{\hat{CF}}\}$, $T_i = \{X(n) : t_i(n) = 1\}$, and E is the subset of RCT.

3.2 Multiple treatment

Unlike the binary treatment problem, the multiple treatment problem can be described by the following stereotype[41]: For each sample, the potential outcomes are represented as a vector Y with N entries Y_j^F where each entry corresponds to the outcome when applying one treatment T_j out of the set of N available treatments $T = \{0, 1, 2, \dots, T_N\}$, with $j \in \{0, 1, 2, \dots, N - 1\}$. The set of available treatments can contain more than two treatments. As training data, samples k and their observed factual outcomes Y^F are received when applying one treatment T_i , the other outcomes can not be observed. The purpose is to train a predictive model \hat{f} that is able to estimate the entire potential outcomes vector \hat{Y} with k entries Y_j .

With the exception of ATE and CATE, an accurate estimate of treatment effect can be determined by using **Root Mean Square Error (RMSE)** for all subgroups, which is defined as[105]:

$$\text{RMSE} = \sqrt{\frac{1}{N} \sum_{n=1}^N \frac{1}{|T|} \sum_{j \in T} (Y^F(n, j) - Y^{CF}(n, j))^2} \quad (7)$$

where T is the set of all possible combinations of treatments, N is the number of observations. $Y^F(n, j)$ displays the true outcome when the j^{th} subset is applied to compute the n^{th} observation, whereas $Y^{CF}(n, j)$ displays the predicted

outcome when the j^{th} subset is applied to compute the n^{th} observation. The **Absolute Error** can be calculated in the same way. This metric is commonly used for the News[41] dataset, which the treatments are the choice of viewing tools, such as smartphones, tablets, desktops, and TVs.

To measure the average of the RMSE between the actual and estimated difference between ITE for each treatment with no treatment ITE, We can incorporate multiple treatments into one calculation criterion, which is called **Average PEHE**[105]:

$$\text{AveragePEHE}_j = \frac{1}{|T|} \sqrt{\frac{1}{N} \sum_{n=1}^N ((Y^F(n, j) - Y^F(n, 0)) - (Y^{CF}(n, j) - Y^{CF}(n, 0)))^2, j \in (T - T_0)} \quad (8)$$

where T_0 represents the sample set with no treatment applied. It is worth mentioning that the latest research on estimating the effect of multi-causal treatment COVID-19[106, 107]. Average PEHE typically serve as performance metrics in dataset CHESS.

3.3 Continuous dose treatment

Vary from binary and multivariate treatment issues, the continuous-dose treatment issue can be formulated as follows[73]: Consider to receive observations of the form $(\mathbf{x}^i, T_f^i, Y_f^i)$ for $i = 1, \dots, N$, where, for each i , these are independent realizations of the random variables (\mathbf{X}, T_f, Y_f) , refer to \mathbf{X} as the feature vector lying in some feature space \mathcal{X} , containing pre-treatment covariates. The treatment random variable, T_f , is in fact a pair of values $T_f = (W_f, D_f)$ where $W_f \in \mathcal{W}$ corresponds to the *type* of treatment being administered which lies in the discrete space of N treatments, $\mathcal{W} = \{w_1, \dots, w_k\}$, and D_f corresponds to the *dosage* of the treatment, which, for a given treatment w lies in the corresponding treatment's dosage space, \mathcal{D}_w (e.g. the interval $[0, 1]$). The set of all treatment-dosage pairs can be defined as $\mathcal{T} = \{(w, d) : w \in \mathcal{W}, d \in \mathcal{D}_w\}$.

In continuous dose treatment situation, the sample dose-response curve⁷ is adopted as the metric. Furthermore, the metric on the test set is different[56]. Therefore, we can use **Mean Integral Squared Error (MISE)** to measure the accuracy of the estimation of the patient treatment effect on the dose space, which is defined as[56].

$$\text{MISE} = \sqrt{\frac{1}{K} \frac{1}{N} \sum_{T_n \in \mathcal{T}} \sum_{n=1}^N \int_{\mathcal{D}_{T_n}} (Y_n(T_n, u) - \hat{Y}_n(T_n, u))^2 du} \quad (9)$$

where T is the set of treatments in the space, K is the number of samples, and u is the treatment dose taken. For a given treatment, T_n lies within the dose space \mathcal{D}_{T_n} . Moreover, $Y_n(T_n, u)$ and $\hat{Y}_n(T_n, u)$ denote the results predicted by the model and the results at the optimal treatment dose, respectively.

In addition, the **Mean Dose Policy Error (DPE)** is another good metric of a model's ability to predict the optimal dose point for each individual treatment, which can be defined by [56]:

$$\text{DPE} = \sqrt{\frac{1}{K} \frac{1}{N} \sum_{T_n \in \mathcal{T}} \sum_{n=1}^N (Y_n(T_n, D_{T_n}^*) - Y_n(T_n, \hat{D}_{T_n}^*))^2} \quad (10)$$

where, $D_{T_n}^*$ and $\hat{D}_{T_n}^*$ represent the true optimal dose and the model-determined optimal dose under a treatment, respectively. With **Sequential Least Squares Estimation**[108], the optimal dose point for the model can be determined.

In order to compare the optimal treatment dose pair selected by the model with the true optimal treatment dose pair, the mean **policy error (PE)** is given as[56]:

$$\text{PE} = \sqrt{\frac{1}{N} \sum_{n=1}^N (Y_n(T_n^*, D_{T_n}^*) - Y_n(\hat{T}_n^*, \hat{D}_{T_n}^*))^2} \quad (11)$$

where T_n^* and \hat{T}_n^* represent the optimal treatment and the optimal treatment determined by the model, respectively. By calculating the optimal dose for each treatment and then selecting the treatment that yields that optimal dose, the optimal dose pair for the model can be selected. The above metrics are typically used in the TCGA[109] dataset. Among them, drug therapy, chemotherapy, and surgery are the treatment options, and the outcome is a risk of cancer recurrence after treatment.

Additionally, many researchers have flexibly applied simulation datasets to differ scenarios. In order to provide more ablation experiments and prove the robustness of the model. A detailed description of the relevant datasets can be found in Section 6.

4 Development of Deep Causal Models

With a solid understanding of the basic definitions and model measures of causal inference, this section moves to the core of the paper. We provide an overview of deep causal models during the last several years and a detailed classification of them.

4.1 A timeline of development

In the past few years, research on deep causal models has advanced considerably, and they have become more accurate and efficient in estimating causal effects. In Figure1, we present the development timeline about 40 classical deep causal models from June 2016 to February 2022.

Deep causal models have emerged since 2016. For the first time, Johansson et al. publish **Learning Representations for Counterfactual Inference**[40], and propose the algorithm framework BNN and BLR[40], in which deep learning is combined with the causal effect estimation, and the causal inference problem is transformed into a domain adaptation problem. Since then, a number of models, including DCN-PD[110], TARNet and CFRNet[42], have been proposed since then. It is important to note that the CEVAE[53] model proposed by Louizos et al. in December 2017, which is based on classical structural **Variational Autoencoders (VAE)**[111], focuses on the impact of confounding factors on the estimation of causal effects.

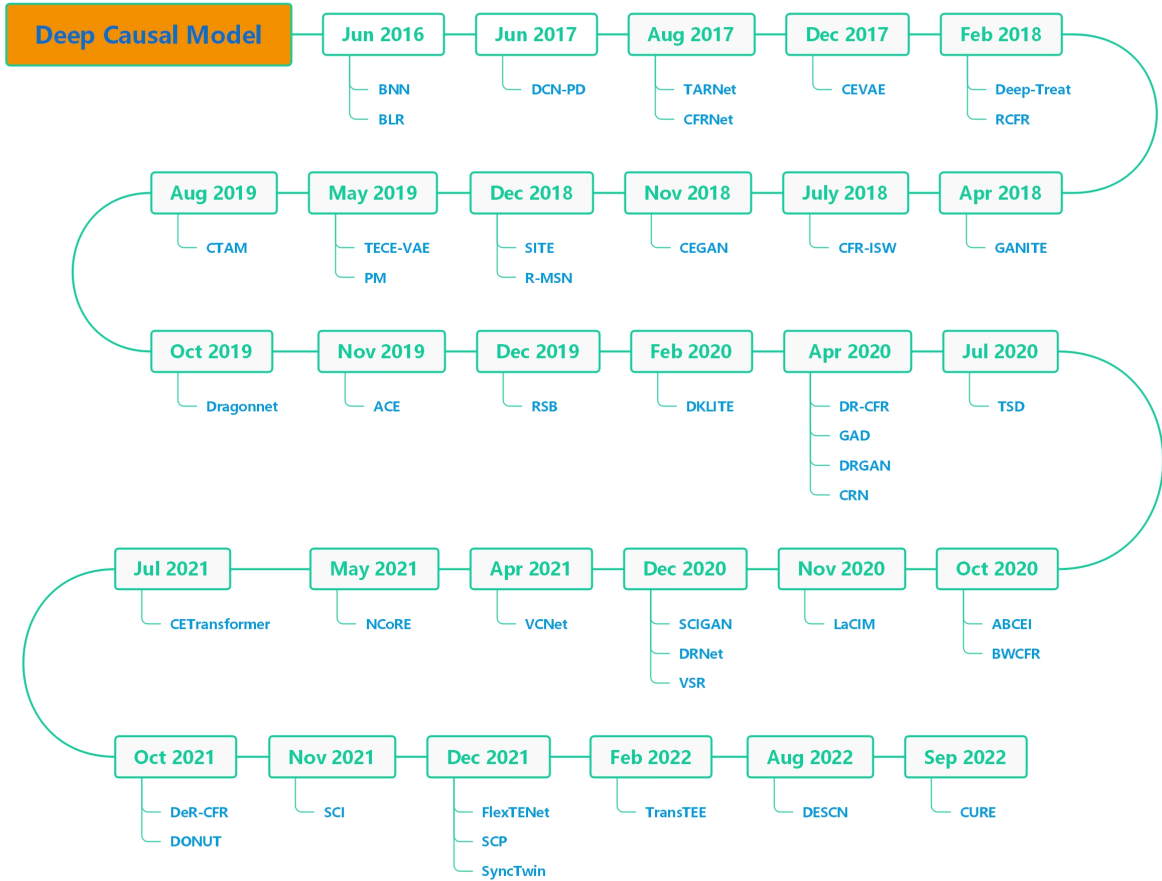


Figure 1: Overview of development timeline of classical deep causal models

In 2018, and going forward into 2019, there emerged an increasing interest in causal representation learning with representative works including Deep-Treat[19] and RCFR[112] models. After the launch of the GANITE[44] model, the use of generative adversarial model[113] architecture for counterfactual estimation becomes mainstream in the field of causal inference. In accordance with the previous works, some novel optimization ideas were proposed in CFR-ISW[114], CEGAN[72], SITE[43].

By applying recurrent neural networks[115], the R-MSN[75] model aims to solve the problem of continuous dose of multi-treatment time series, which opened up a new theory of deep causal models. Furthermore, PM[41] and TECE-VAE[105], proposed in 2019, attempt to address the issue of estimating causal effects associated with multiple discrete treatments. As a follow-up, the CTAM[33] begins to focus on estimating causal effects for textual data; the Dragonnet[70] adhibits regularizations and propensity score networks into causal models for the first time; the ACE[54] attempts to extract fine-grained similarity information from representation space. After that, RSB[116] model adopts deep representation learning network and PCC[117] regularization for covariate decomposition, uses instrumental variables to control selection bias, and uses confounding factors and moderating factors to predict results.

In 2020, deep causal models got a rapid boom. For DKLITE[55] model, it effectively combines the deep kernel trick and posterior variance regularization. Then, DR-CFR[118] was proposed to decouple selection bias for covariates; GAD[119] focuses on the causal effect of continuous dose treatment; DRGAN[120] defines an innovative generative adversarial network for fitting sample dose effect curves; and CRN[121] estimates time-varying treatment effects by combining counterfactual recurrent neural networks. Following estimating time series causal effects under multi-cause confounding, TSD[122] turns to the estimation of time series causal effects. In the aspect of learning the latent representation space, ABCEI[123] achieves a good balance between the covariate distribution of treatment and the control groups by using GAN. As two variants of previous works[42, 53], both BWCFR[124] and LaCIM[125] are further optimized for the model structure. Additionally, in 2020, SCIGAN[73] and DRNet[56] extended the task of continuous dose treatment to arbitrary quantity, while VSR[126] aggregated the deep latent variables in a reweighted manner.

Up to now since 2021, deep causal models have become more innovative, open, and flexible. The VCNet[57] model implemented an estimator of continuous mean dose-response curves. As for NCoRE[127], it used cross-treatment interaction models to explain the process of multi-treatment combination at the potential causal level. After that, inspired by the success application of Transformer [128] in many fields, CETransformer[129] was proposed to characterize the covariates by focusing the attention on the correlation between the covariates. In addition, DONUT[130] and DeR-CFR[69] are optimized for the two previous works[70, 118] respectively. In [76], the subspace methods was further explored for causal representation learning, which formulate the SCI model. From the perspective of multi-task learning e, a multi-task adaptive learning architecture was proposed by FlexTENet[131], in which CATE estimation architecture adaptively learns what to share between the PO functions. Aside from that, SCP[132] attempted to estimate the multifactorial treatment effects using a two-step procedure. To construct synthetic twin matching representation, SyncTwin[101] utilized the temporal structure in the potential outcomes. In 2022, TransTEE[77] extended the distribution balance approach for spatial representations to continuous, structured, and dose-dependent treatments, applying the latest theory of deep learning to expand the depth and breadth of causal inference. Furthermore, DESCN[133] obtained comprehensive information on treatment propensity, response and hidden treatment effects through a crossover network by means of a multi-task learning. Until recently, CURE[134] pre-trained large-scale unlabeled patient data to learn representative background patient representations, and then fine-tunes the labeled patient data for treatment effect estimation.

4.2 Model classification

Through sorting out the existing models, we can find that the current deep causal models are mainly studied from the following aspects that include : 1) Learning balanced representations; 2) Covariate confounding learning; 3) Time series causal learning; 4) GANs based Counterfactual simulation; and 5) Multi-treatment and continuous-dose treatment. In Figure 2, we present a detailed classification of the current deep causal model.

- **Learning balanced representations:** This type of approach has long been a popular research. The core ideology is to use the encoder to map the covariates X to the representation space Φ , combine the processing T , adopt the network h to predict the output outcome Y , and minimize the distribution distance $\text{disc}_{\mathcal{H}}$ between the factual and counterfactual outcomes. Classical architectures include BNN[40], CFRNet[42], SITE[43], ACE[54], DKLITE[55], SCI[76], etc.
- **Covariate confounding learning:** This type of approach aims to decomposition of covariant relation in theory. Its main application schemes are unbiased estimation of covariates and removal of confounding factors using decoupling, reweighting, codec reconstruction, etc. The typical structures include CEVAE[53], Dragonnet[70], DeR-CFR[69], LaCIM[125], DONUT[130], FlexTENet[131], and so on.
- **GANs-based counterfactual simulation:** With the great success of GANs in data synthesis in recent years, it is also widely adopted to solve causal effect estimation problems. Two schemes are usually involved in Using GAN networks for counterfactual simulation, i.e., generating the counterfactual output outcomes or balanced representation space distributions. Such classical frameworks include GANITE[44], CEGAN[72], ABCEI[123], CETrnaformer[129], etc.

- **Time series causal estimation:** Temporal causal estimation has been widely concerned. Using RNNs to track contextual covariate information and handle time-varying confounding bias is a long-standing solution adopted by many models. Some typical architectures are R-MSE[75], CTAM[33], CRN[121], TSD[122], and so on.
- **Multi-treatment and continuous-dose treatment:** The issues of Multiple treatment and continuous-dose treatment are one of recent research hotspots in deep causal learning. In general, such issues can be further simplified and structured using schemes such as matching, variational autoencoders, hierarchical discriminators, and multi-headed attention mechanisms. The classical models include PM[41], TECE-VAE[105], DRNet[56], SCIGAN[73], VCNet[57], TransTEE[77], etc.

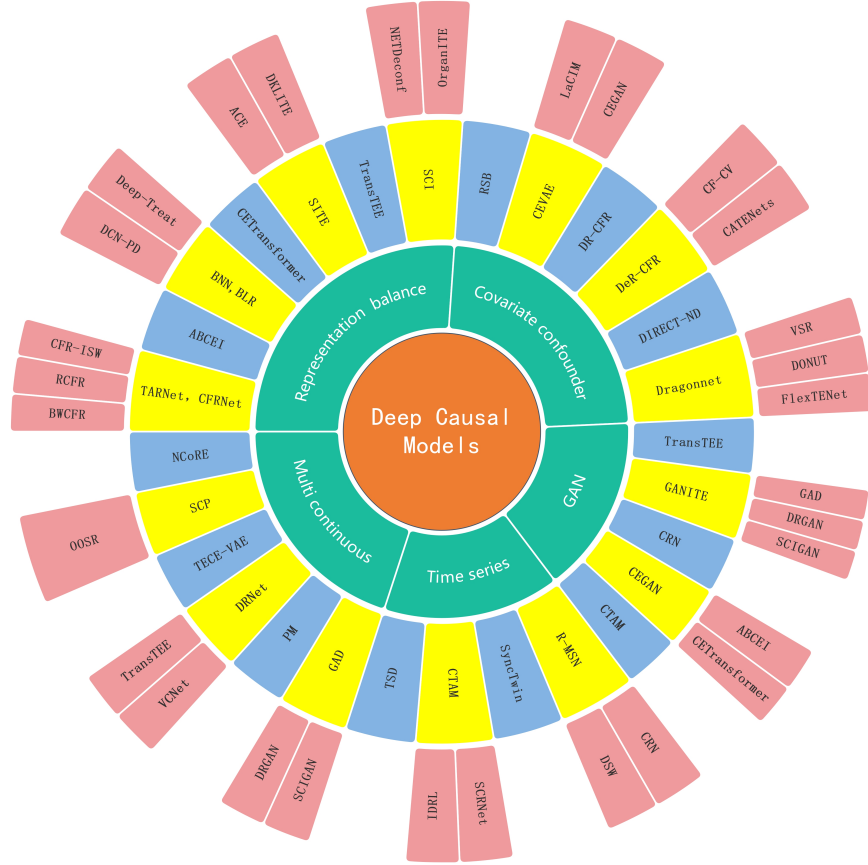


Figure 2: **Taxonomy of deep causal models**

It is worth pointing out, as different application scenarios arise, new research focuses and methods in the aspect of deep causality model will also emerge continuously. In the following section, we will give a detailed introductions to the typical models according to the taxonomy of deep causal models motioned above.

5 Typical Deep Causal Models

As more and more data accumulate in the fields of healthcare, education, economy, etc., deep learning is increasingly being used to infer causal relationships from counterfactual data. As opposed to existing deep causal models, which typically map covariates to a representation space, unbiased estimation of counterfactual data can be achieved by the objective function. Unlike the brief overview of the various classical models that are categorized from the different research perspectives for deep causal models, Table 2 summarizes the classical network architecture applied by those typical deep causal models. In addition, in the following detailed descriptions on the typical deep learning-based causal models, the issues and challenges that these models face are also discussed.

| Models | GAN | AE | RNN | Transformer |
|--------------------|-----|----|-----|-------------|
| DCN-PD[110] | × | × | × | × |
| BNN[40] | × | ✓ | × | × |
| CFRNet[42] | × | ✓ | × | × |
| CEVAE[53] | × | ✓ | × | × |
| Deep-Treat[19] | × | ✓ | × | × |
| GANITE[44] | ✓ | × | × | × |
| CEGAN[72] | ✓ | × | × | × |
| SITE[43] | × | ✓ | × | × |
| R-MSN[75] | × | × | ✓ | × |
| PM[41] | × | ✓ | × | × |
| TECE-VAE[105] | × | ✓ | × | × |
| CTAM[33] | ✓ | ✓ | × | × |
| Dragonnet[70] | × | ✓ | × | × |
| ACE[54] | × | ✓ | × | × |
| RSB[116] | × | ✓ | × | × |
| DKLITE[55] | × | ✓ | × | × |
| GAD[119] | ✓ | × | × | × |
| CRN[121] | ✓ | × | ✓ | × |
| TSD[122] | × | × | ✓ | × |
| ABCEI[123] | ✓ | ✓ | × | × |
| BWCFR[124] | × | ✓ | × | × |
| LaCIM[125] | × | ✓ | × | × |
| SCIGAN[73] | ✓ | ✓ | × | × |
| DRNet[56] | × | ✓ | × | × |
| VSR[126] | × | ✓ | × | × |
| VCNet[57] | × | ✓ | × | × |
| NCoRE[127] | × | ✓ | × | × |
| CETransformer[129] | ✓ | ✓ | × | ✓ |
| DeR-CFR[69] | × | ✓ | × | × |
| SCI[76] | × | ✓ | × | × |
| WUNT[135] | × | × | × | ✓ |
| FlexTENet[131] | × | ✓ | × | × |
| SCP[132] | × | ✓ | × | × |
| CGN[74] | ✓ | ✓ | × | × |
| SyncTwin[101] | × | × | ✓ | × |
| TransTEE[77] | ✓ | ✓ | × | ✓ |
| DESCN[133] | × | ✓ | × | × |
| CURE[134] | × | ✓ | × | ✓ |

Table 2: **Highlights of deep frameworks on classical causal models**

5.1 Learning balanced representation

Most statistical learning theories posit that the test data and training data have independent and identical distributions, but in reality, the distributions of test data and training data are often related, but not identical. Solving this problem requires deep learning models that learn causality rather than correlation in the field of causal inference. There is no standard treatment assignment strategy for observational data, unlike RCTs. As we know, fact and counterfactual distributions are often different because of selection bias caused by known and unknown covariates. Hence, causal

inference needs to be transformed into a domain adaptation problem to predict counterfactual outcomes by learning from factual data.

For counterfactual results to be predicted, effective feature representations are necessary, especially the balanced distributions. According to Johansson et al, BNN[40] is an algorithmic framework as shown in Figure 3 for counterfactual reasoning that transforms the causal inference problem into a representation distribution balance problem.

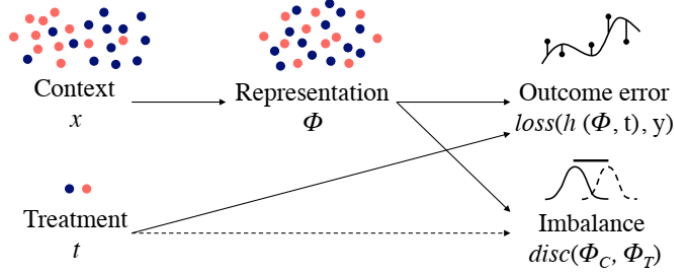


Figure 3: **Balancing Neural Network (BNN)** [40]: Counterfactual inference networks based on representation distribution balance

Upon mapping the covariates to the representation space, the encoder makes use of a two-layer fully connected neural network, balances the distribution distance of the representation space, and then derives the counterfactual results using another two-layer fully connected network. The used regression function is as follows:

$$B_{\mathcal{H}, \alpha, \gamma}(\Phi, h) = \frac{1}{n} \sum_{i=1}^n |h(\Phi(x_i), t_i) - y_i^F| + \alpha \text{disc}_{\mathcal{H}}(\hat{P}_{\Phi}^F, \hat{P}_{\Phi}^{CF}) + \frac{\gamma}{n} \sum_{i=1}^n |h(\Phi(x_i), 1 - t_i) - y_{j(i)}^F| \quad (12)$$

where the encoder network is represented by Φ , a predictor network by h , and the metric function is $\text{disc}_{\mathcal{H}}$ that represents the distance between the two distributions. Aside that, Eq.(12) minimizes the error of the training set facts.

As an innovative method for measuring the spatial distribution distance between treatment groups and control groups, the literature[42] proposed a CFRNet network structure based on BNN[40] and adopted MMD[136] and WASS[137, 138] for spatial distribution distance representations. When the network is trained, the imbalance penalty is calculated based on the explicit boundary of the distance, and the loss is calculated separately for the treatment group and the control group. As well as adding multiple neural network layers between results prediction layer, DCN-PD[110] combined multi-task deep neural networks with propensity score dropout[139].

On the basis of the CFRNet[42] model, both RCFR[112] and CFR-ISW[114] used the Propensity score[140] to re-weight the representative spatial feature region and the sampling objective function; Atan et al. proposed an unbiased autoencoder network Deep-Treat[19] framework, applying a feedforward neural network to learn the optimal treatment strategy. While it reduces the loss of representation reconstruction as well as the information loss in space, the selection bias is also narrowed.

To maintain local similarity and balance of data representing the treatment and control groups and to improve individual treatment outcomes. Yao et al. proposed the SITE[43] method, which combines position-dependent depth metric PDDM with midpoint distance minimization MPDM into the representation space, and predicts the potential outcomes using a binary result network. In this case, the following loss function is used:

$$\mathcal{L} = \mathcal{L}_{\text{FL}} + \beta \mathcal{L}_{\text{PDDM}} + \gamma \mathcal{L}_{\text{MPDM}} + \lambda \|W\|_2 \quad (13)$$

where \mathcal{L}_{FL} is the loss between the predicted and observed factual outcomes, $\mathcal{L}_{\text{PDDM}}$ and $\mathcal{L}_{\text{MPDM}}$ are the loss functions of the PDDM and MPDM, respectively, and the last term is the L_2 regularization of the model parameter M .

According to SITE[43], ACE[54] proposed a balanced and adaptive similarity regularization structure to extract spatially fine-grained similarity information; in [55] DKLITE was proposed by applying the deep kernel regression and a posterior regularization to learn the spatial domain overlap information; and BWCFR[124] re-weighted the spatial feature distribution for the domain overlap region.

Unlike the above models, many other works attempt to combine representation distribution balancing with other deep network models. By combining a GAN[113] network with a mutual information estimator regularization structure, ABCEI[123] tries to balance the covariate distributions of the treatment and control groups in the representation space; In [129], CETransformer was proposed to apply the attention mechanism to focus on the relationships between

covariates and then learn a balanced representation distribution; As TransTEE[77] extends the balanced representation distribution method to Continuous, Structured, and Dose-Related treatments, it makes causal effect estimation a more open-ended problem; CURE[134] designed a new sequence encoding for longitudinal (or structured) patient data and merge structure and time into patient embeddings; DESCN[133] learned the processing and response functions jointly across the sample space to avoid processing bias, and used an intermediate pseudo-processing effect prediction network to mitigate sample imbalance; In [76], SCI induced the concept of a subspace as shown in Figure 4, integrating the covariates into a common subspace, a treatment subspace, and a control subspace simultaneously, thereby obtaining a common representation and two specific representations. Afterwards, the common representation is connected to the specific representation of the treatment group and of the control group, and two potential results are obtained from the reconstruction and prediction network. Based on SCI, NETDECONF[102] used network structure information to infer hidden confounding in the observational data. A personalized treatment effect model that allocates treatments according to scarcity and estimates potential outcomes is proposed by OrganITE[141].

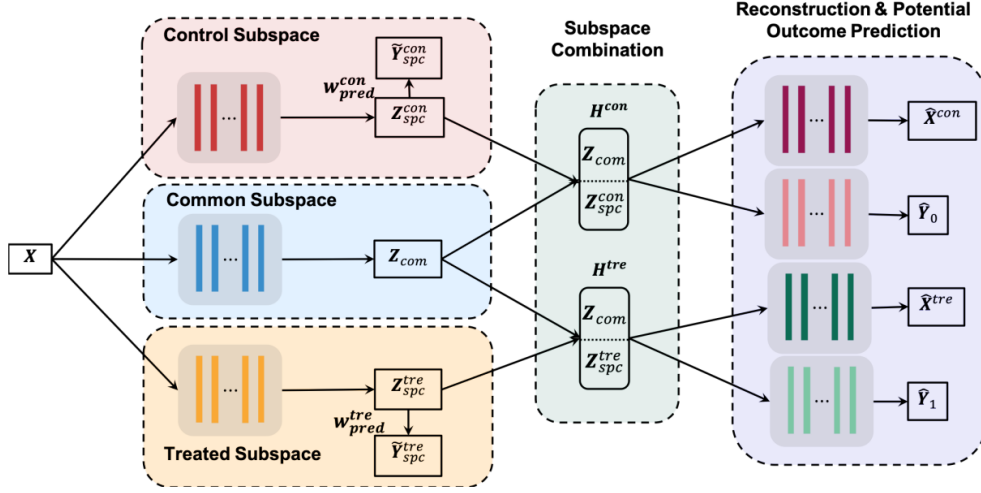


Figure 4: **Subspace Learning Based Counterfactual Inference network (SCI)** [76]: Estimating individual causal effects while preserving information about specific and common subspaces

Due to the improvement in the feasibility of estimating causal effect, the representation distribution balance is becoming the mainstream way, but it is still limited to estimating individual treatment effects, and thus is hard to expand to a broader range of applications like multi-treatments and continuous-dose treatments.

5.2 Covariates confounding learning

The main issue in causal inference is estimating the treatment effect when given a covariate, a treatment, and a predicted outcome. By identifying and correcting for confounders, it is possible to estimate causal effects with greater accuracy from observational data. Nevertheless, in practical cases, there are potential confounders of noise and uncertainty, as well as some non-confounders. For this reason, mining potential confounders and decoupling the associated covariates are important methods to learn unbiased representations of counterfactuals from observed data.

A CEVAE[53] model structure was first proposed by Louizos et al. to capture hidden confounding factors with VAEs [142, 143] in the presence of noise and uncertain confounding factors, and perform treatment and prediction. The causal correlation diagram is shown in Figure 5. The meaning of the graph can be expressed as follows: t represents for the drug treatment, y for the mortality, z for the socioeconomic status, and x for the income and place of residence in the past year, respectively.

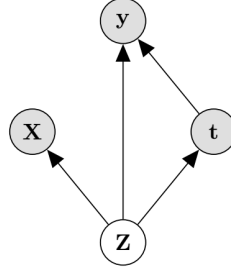


Figure 5: **Causal Effect Variational Autoencoder (CEVAE)** [53]: Cause-and-effect diagram

On the basis of TARNet[42]’s causal relationship diagram structure, Do-calculus[144] derivations are performed for y and t in the inference network, respectively, and z and t in the model network to fit the interaction between potential confounding variables and treatment effects. Overall, the following prediction function is involved in the causal variational autoencoder:

$$\mathcal{F}_{\text{CEVAE}} = \mathcal{L} + \sum_{i=1}^N (\log q(t_i = t_i^* | \mathbf{x}_i^*) + \log q(y_i = y_i^* | \mathbf{x}_i^*, t_i^*)) \quad (14)$$

where, in the training set, the input, treatment, and outcome random variables are observed at points \mathbf{x}_i^* , t_i^* , and y_i^* , respectively.

On the ground of CEVAE[53], Sun et al. proposed the LaCIM[125] latent causal model to avoid false associations and improve the generalization ability of the model; CEGAN[72] used GAN networks to identify the potential confounders unbiasedly.

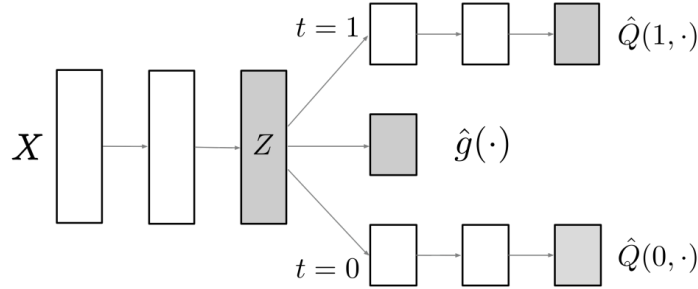


Figure 6: **Dragonnet**[70]: Propensity score adaptive neural network

Proposed by Shi et al., first-ever Dragonnet[70] adhibited the regularization objective functions into nonparametric estimation theory and the Propensity score prediction networks to CFRNet[42], thus making sure that the covariates are adjusted for treatment-related information in them. As can be seen, Figure 6 shows the network structure of the propensity score adaptive neural network. In accordance with Dragonnet[70], VSR[126] proposed a reweighting model that removes the association processing and confounding factors. It also used a deep neural network to aggregate the density ratios of latent variables across the variational distribution for calculateing the sample weight distribution; As part of the estimation process, DONUT[130] has added an orthogonal constraint to the non-confounding factors in the total loss; In addition, an end-to-end regularization and reparameterization method called FlexTENet[131] was proposed to learn a new architecture using multi-tasking framework, by which the shared function between causal structures is obtained adaptively. In DIRECT-ND[145], the entangled representation is solved through hybrid learning, and the multivariate causal effect estimation problem was studied from a new perspective. Additionally, VAE and GAN networks were added to the model to realize the learning of hybrid representation space.

Aiming at balancing selection bias, Zhang et al. [116] proposed the RSB algorithm using autoencoder networks via PCC regularization and instrumental variables, and also adding the confounding variables and moderators for prediction. As extention of CFRNet[42], both , DR-CFR[118] and DeR-CFR[69] were proposed with the main structure as shown in Figure 7 to remove the covariate correlations.

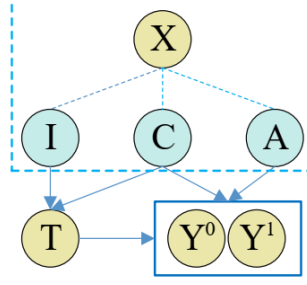


Figure 7: **Decomposed Representation for CounterFactual Regression (DeR-CFR)** [69]: Causal framework with decomposed latent factors

As we can find from Figure 7, there are three possible factors contributing to the observed covariates X in the figure. The instrumental factor I , which only affects the treatment T ; the confounding factor C , which causes the outcome Y along with the treatment T ; and the adjustment factor A , which determines the outcome Y . Learning the decomposed representation for counterfactual reasoning consists of the following steps[69]:

- Three decomposed representation networks for learning latent factors, one for each underlying factor: $I(X)$, $C(X)$, and $A(X)$.
- Three regularizers for confounder identification and balancing are: the first is to decompose A from X by considering $A(X) \perp\!\!\!\perp T$ and $A(X)$ should predict Y as accurately as possible; the second is to decompose I from X by constraining $I(X) \perp\!\!\!\perp Y \mid T$, and $I(X)$ should be predictive of T , based on Assumption 2; the last is designed for simultaneously balancing confounder $C(X)$ in different treatment arms.
- Two regression networks for potential outcome prediction, one for each treatment arm: $Y^0(C(X), A(X))$ and $Y^1(C(X), A(X))$.

The following is the orthogonal regularizer function used in the decomposition process:

$$\mathcal{L}_O = \bar{W}_I^T \cdot \bar{W}_C + \bar{W}_C^T \cdot \bar{W}_A + \bar{W}_A^T \cdot \bar{W}_I \quad (15)$$

To prevent the representation network from rejecting any input, the sum of \bar{W}_I , \bar{W}_C and \bar{W}_A are constrained to be one. For a hard decomposition, the orthogonal regularizer ensures each variable in X can only flow into one representation network.

Based on DeR-CFR, CATE’s prediction performance has been assessed using CF-CV[146], which selects the best model or hyperparameters from potential candidates. In [147], a meta-learning approach was combined together with deep networks, theoretical reasoning, and the optimal counterfactual information.

Causative treatment effect estimation has always been concerned with rationally using confounding variables. The decoupling of covariates to learn related confounding variables can help remove selection bias and generate unbiased output estimates. Despite its theoretical nature, this kind of methods has also some limitations in practical applications, as it requires decomposing covariates into reasonable explanations.

5.3 GANs-based counterfactual simulation

In deep generative models, generative adversarial networks (GANs)[113] can capture the uncertainty of counterfactual distributions. The generator produces counterfactual results or consistency distribution between control and treatment groups, while the discriminator fits the unbiased estimation of the treatment effects. As well as using factual data, GAN networks also consider the accuracy of counterfactual results when making causal inferences. In light of this, generative adversarial models are increasingly used for causal effect estimation.

The first approach suggested by Yoon et al. is for the GANITE[44] network to generate the counterfactual results based on factual data and pass them to the ITE generator. Figure 8 shows the detailed block diagram of GANITE.

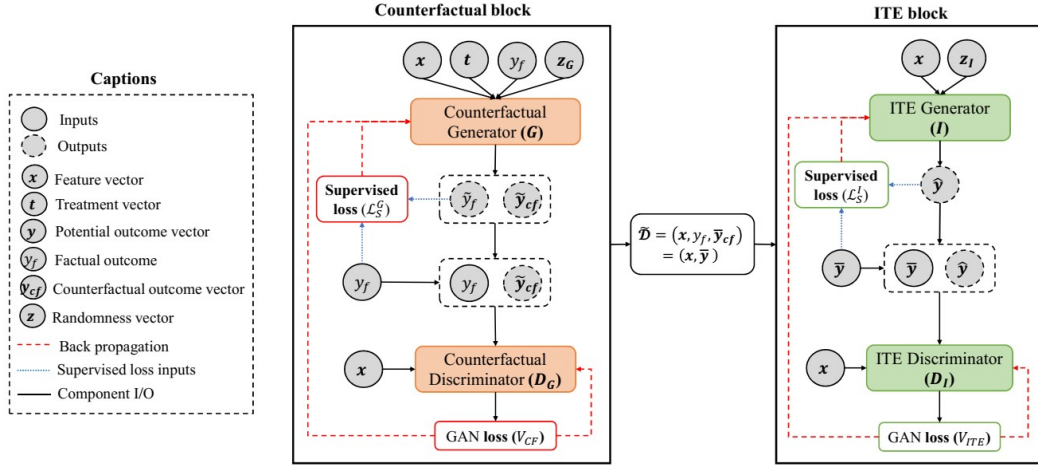


Figure 8: **Generative Adversarial Nets for inference of Individualized Treatment Effects (GANITE)** [44]: Block diagram

For a given feature vector x , GANITE generates the potential output results by first generating factual outputs y_f and then counterfactual samples y_{cf} using generator G . After these counterfactual data are combined with the original data, a complete data set \tilde{D} is generated in generator I of the ITE module, which then optimizes \tilde{D} , yielding an unbiased estimate of each treatment's effect.

For the first time, CEGAN[72] has applied the GAN network to balance the distributions between the spatial treatment group and the control group by leveraging the discriminative loss of the GAN network and weighting the Decoder's construct loss or weight after the Encoder. In order to solve the generator-discriminator min-max problem, the following reward function is used:

$$\min_{(\theta_E, \theta_I, \theta_P)} \max_{\theta_D} \mathbb{E}_{q_E(\mathbf{z}, \mathbf{x}, t, \mathbf{y})} [\log(D(\hat{\mathbf{z}}, \mathbf{x}, t, \mathbf{y}))] + \mathbb{E}_{q_P(\mathbf{z}, \mathbf{x}, t, \mathbf{y})} [\log(1 - D(\mathbf{z}, \mathbf{x}, t, \hat{\mathbf{y}}))] \quad (16)$$

where the encoder-decoder's joint distribution is represented by $q_E(\mathbf{z}, \mathbf{x}, t, \mathbf{y})$ and $q_P(\mathbf{z}, \mathbf{x}, t, \mathbf{y})$, while their probability estimations are represented by $(D(\hat{\mathbf{z}}, \mathbf{x}, t, \mathbf{y}))$ and $(1 - D(\mathbf{z}, \mathbf{x}, t, \hat{\mathbf{y}}))$, respectively. The discriminator determines which distribution the samples belong to.

In addition to GANITE and CEGAN, there are also many works using GAN networks to estimate the causal effects in other fields. As part of a generative adversarial framework, GAD[119] applied GAN networks to continuous treatment problems to learn a sample-balanced weight matrix, which removes the association between treatment regimens and covariates; to address multiple treatments as well as consecutive doses treatment problems, DRGAN[120] proposed a model architecture consisting of a counterfactual generator, discriminator, and inference block; As a means of better coping with continuous intervention problems, SCIGAN[73] added a hierarchical discriminator based on DRGAN. In addition, CTAM[33] has also applied the generative adversarial ideas to the treatment effect estimation of text sequence information,. It filters out information related to approximate instrumental variables when learning representations, and matches between the learned representations; To eliminate the association between the treatment and patient history, CRN[121] utilized a counterfactual recurrent neural network to reflect the time-varying treatment effect; In ABCEI[123], the covariate distributions between the control and treatment groups are well balanced with GAN networks, and a regularization function of mutual information estimators is added to reduce bias; To learn the balanced covariate representations, CETransformer[129] combined the attention mechanism with WGAN; In TransTEE[77], Transformer[128] was used for covariate representation, in which the treatment effectiveness is estimated by the Propensity Score Network and the selection bias can be overcome by the GAN network. In particular, the model can also be used for discrete, continuous, structured or dose-related treatments.

In general, it is not hard to extend the ways of individual treatment effect estimation to multiple interventions and continuous dose interventions using the GAN network, and it has a good effect on the balance of representation distribution and the generation of potential results. However, due to lacking a complete theoretical support system, using GAN networks to solve the problem of causal effect estimation requires more impeccable theoretical derivation in the future.

5.4 Time series causal estimation

In treatment effect estimation, most models focus on numerical variables, and it is still difficult to deal with textual information and time series information[148]. Variable decoupling for textual information estimation can reduce estimation bias since there are many covariates in textual information that are unrelated to causal effect estimation. When dealing with time-series information, RNNs[115] have usually been combined to create counterfactual recurrent networks based on historical information.

The R-MSN[75] model is first proposed by Lim et al. in order to address the problems arising with continuous treatment doses and multi-treatments under time series. Figure 9 illustrates the model's frame structure, which uses a recurrent edge network to remove time-dependent confounding, an a standard RNN structure to encode and decode.

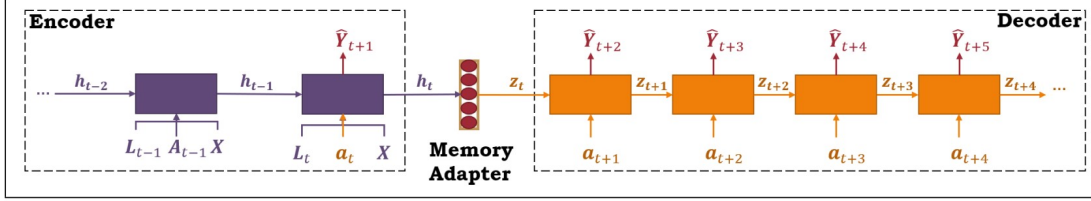


Figure 9: **Recurrent Marginal Structural Network (R-MSN) [75]:** Architecture for multi-step treatment response prediction

To predict the causal effect, R-MSN used the standard LSTM[149] structure, dividing multi-treatment and continuous intervention problems according to the corresponding time interval. As a counterfactual recurrent network, CRN[121] constructs a treatment-invariant representation for each time step based on R-MSN[75], eliminating the patient's medical history association between treatment allocation and treatment allocation and balances time-varying confounding biases; By combining with the current treatment assignment and historical information, the hidden confounders are inferred using recurrent weighted neural networks in DSW[150], an then reweighted using time-varying inverse probabilities. In addition to building a multi-task output RNN factor model, TSD[122] allocates multiple treatments over time, an then estimates the treatment effects with multi-cause hidden confounders by which the latent variables free of treatment can be inferred. Furthermore, it substitutes the unobserved confounders with latent variables, and infers logistic regression results in the absence of treatment; In SyncTwin[101], treatment estimation is performed based on the temporal structure of the prediction results, and synthetic twin samples are constructed and counterfactual predictions are obtained.

Yao et al. proposed a matching treatment-adversarial learning CTAM[33] method that takes into account text sequence information. As shown in Figure 10, when learning representations, it filters out the approximate instrumental variables and then makes matching between the learned representations to estimate the treatment effect.

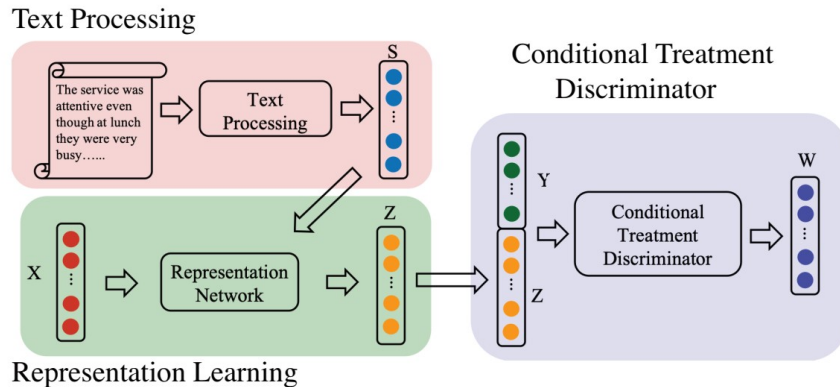


Figure 10: **Conditional Treatment-Adversarial learning based Matching Method (CTAM) [33]:** Framework

Specifically, there are three main components of CTAM[33]: text processing, representation learning, and conditional treatment discrimination. In the first step, the text processing part transforms the original text into a vector representation

S , concatenates S with non-text covariates X , and then constructs a unified feature vector that transforms the input into the latent representation Z . As a next step, both Z and Y are fed into the conditioned treatment discriminator, and during the training process, a max-minimum arithmetic unit is calculated between the representation learning network and the conditioned treatment discriminator. In order to filter out information related to instrumental variables, the representation learning network prevents the discriminator from assigning the correlative treatment. As a last step, it implements the match in the representation space Z .

To predict treatment assignment using mutual information between global feature representations and individual feature representations, IDRL[151] proposed to learn Infomax and domain-independent representations. To maximize the ability of capturing the common prediction information among treatment and control groups, the influence of instrumental variables and irrelevant variables were filtered out. In addition, the SCRNet[152] attempted to estimate ITE with different types of variables by dividing the covariates.

Estimation of causal effects of textual time series is often combined with the problems related to multiprocessing and continuous dose processing. Despite the widespread application of this direction, researchers need to develop a standard for measuring intervention effects based on the actual situation, and it is difficult to assess the rationality and reliability of the various working standards used in the industry.

5.5 Multi-treatment and continuous-dose models

Casual estimation for individual treatments focuses on solving binary treatment problems, and extending it to multiple treatments is computationally expensive. However, multiple treatments and continuous-dose models have many applications, such as radiotherapy, chemotherapy and surgery for cancer treatment, as well as prolonged usage of vasopressors[100] for many years. It is therefore beneficial to estimating the effects of ongoing interventions in these various treatment settings in order to make good long-term process decisions.

For the first time, Schwab et al. have extended individual treatment estimation to multi-discrete treatment problems with the PM[41] algorithm. In PM, counterfactual reasoning is utilized in small batches by matching nearest neighbors samples, which makes it easily implemented and is compatible with a wide range of architectures, and there is no need to increase computation complexity or other hyperparameters for treating arbitrary quantity of patients. In order to capture higher-order effects, TECE-VAE[105] modeled the dependence between treatments by using task embedding, extending the problem to arbitrary subsets of multi-treatment situations.

When solving problems involving multi-treatments and continuous-dose treatments, GAN networks are frequently combined. A two-step generative adversarial de-aliasing algorithm proposed by GAD[119] can be used for continuous treatment problems, removing the association between covariates and treatment variables. Specifically, it is along with the following three steps: A) Produce an unbiased distribution with no correlation between the covariates; B) Learn the sample weights and transfer the observed data to the unbiased distribution; C) De-obfuscate the data with generative adversarial networks.

As an improved GAN model, DRGAN[120] takes the form of a generator, a discriminator, and prediction network to generate a complete dose-response curve for each sample by considering both multi-treatment and continuous-dose treatment options; By using a hierarchical discriminator on the basis of DRGAN, SCIGAN[73] was proposed to improve the model's ability of handling the problems of continuous intervention.

Meanwhile, a set of open model benchmark parameters, including MISE, DPE, PE, and model selection criteria, were proposed in DRNet[56], which allows the generation of dose-response curves for an unlimited number of treatments under continuous dose parameters. In VCNet[57] that utilizes a variable coefficient neural network, a continuous ADRF[153, 154, 155] estimator is automatically calculated for the continuous activation function, which is helpful of preventing the processing information from being lost. Moreover, the existing target regularization method was also extended to obtain a double robust ADRF curve estimator.

As part of DRNet[56], continuous treatments are divided into blocks and trained separately into hidden layers, which are then nested into each other to construct a piecewise fit of individual dose-response curves; A continuous prediction head of weighted treatment is created by VCNet[57] by paying closer attention to treatment continuity, and optimizing the individual prediction head into a mapping function of covariates that change with treatment. The structure comparison of DRNet and VCNet models is shown in Figure 11.

TransTEE[77] combines the hierarchical discriminator of SCIGAN[73] with the variable coefficient structure of VCNet[57] and induces the Transformer multi-headed attention mechanism generic framework to extend the causal effect estimation problem to discrete, continuous, structured, and dose-related treatments.

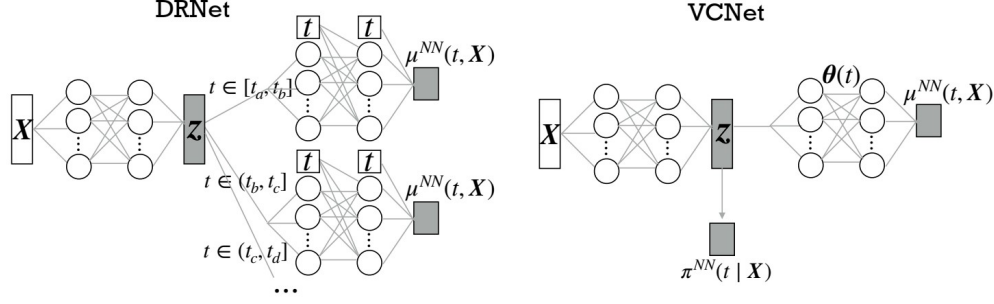


Figure 11: **Dose Response Network (DRNet)** [56] and **Varying Coefficient Neural Network (VCNet)** [57]: Comparison of network structures

As the first study of the multi-treatment combination problem, NCoRE[127] has used the cross-treatment interaction to infer the causal generative processes underlying multiple treatment combinations, in which the counterfactual representations learned in a treatment setting are combined.

To estimate the multi-cause perturbation treatment effect, Prichard et.al proposed the idea of SCP[132] for the first time. To overcome the confounding bias in two steps, a single-cause CATE estimator is first applied to augment observed data and estimate potential outcomes; As a next step, the augmented data set is adapted for covariates to obtain multi-factor unbiased estimators. In addition to illustrating the relationship between single-factor and multiple-factor problems, SCP shows the equivalence of conditional expectations of single-factor interventions and multiple-factor interventions, which can be verified by the following equation:

$$\mathbb{E}_{\alpha} (Y(a_k, \mathbf{a}_{-k}) | \mathbf{X}) = \mathbb{E}_k (Y(a_k) | \mathbf{X}, \mathbf{A}_{-k}(a_k) = \mathbf{a}_{-k}) \quad (17)$$

In the first step of augmenting the dataset, outcomes and observations $Y(a_k)$ and $\mathbf{A}_{-k}(a_k)$ are added. As such, by training a supervised learning model on the augmented dataset, it is possible to estimate the expected value on the right side of Eq. 17 as well as the multifactorial intervention effect given by the left side in a way that enhances the generalizability of the estimator. In contrast to SCP, OOSR[156] proposed a prediction model using a reweighting way that puts emphasize on the outcome-oriented treatment.

Recently, more and more researchers have taken interest in the problem of multi-treatment and continuous dose therapy, and have also made significant contributions. Nevertheless, there are still many models in this area that need to be developed. Especially, it is still an urgent issue to solve how to formulate a unified causal effect measurement standard.

6 Guideline for Experiment

After an in-depth description of the deep causal modeling approach, this section will provide a detailed experimental guide, including a comprehensive conclusion and analysis of datasets, source codes as well as experiments.

6.1 Datasets

As counterfactual results can never be observed in real life, finding datasets that satisfy experimental requirements is difficult. Most of the datasets used in the literature are semi-synthetic. Following the survey[2], we further supplemented in Table 3 more relevant datasets that are popularly used for causal analysis. Meanwhile, we also conclude the application scenarios for these datasets. In addition, Table 4 summarizes the web links to these datasets and the classical models that are evaluated on them. Below are the detailed descriptions of the available datasets.

IHDP. the Infant health and development[104] dataset was generated from a randomized controlled trial of preterm infants with low birth weight. Various features of the children and their mothers are measured as pre-treatment covariates, such as birth weight, head circumference, neonatal health index, prenatal care, mother’s age, education, drugs, and alcohol. Intensive high-quality childcare is presented to infants in the treatment group, such as specialist home visits[157]. The outcome is a score on the cognitive test for the infant. Moreover, noisy subsets of treatment groups need to be removed to build unbiased selection models.

Jobs. The employment dataset studied by Jobs in LaLonde (1986)[91] is composed of randomized data based on state-supported work programs and nonrandomized data from observational studies. The pre-treatment covariates

include eight variables such as age, education, race, and income in 1974 and 1975. The treatment group has taken part in the vocational training, while the control group has't. The outcome is the employment status.

Twins. The Twins dataset comes from data on twin births in the United States from 1989-1991[158]. An evaluation of 40 covariates pertaining to pregnancy, twin births, and parents is carried out for every pair of twins, including gestational weeks just before birth, quality of care during pregnancy, pregnancy risk factors (anemia, alcohol, smoking, etc.), nursing, residence, and more. The outcome is a one-year mortality rate. A twin dataset is available with results from the treatment (heavier of the twins) and control groups (lighter of the twins). Selection bias is typically simulated by assigning different treatments based on user-defined criteria.

News. The News dataset consists of 5000 randomly sampled news articles from the New York Times corpus. The news dataset contains data on media consumers' perceptions of news items. A sample is a news item consisting of word counts, the results are readers' opinions, and the treatments are a variety of devices that can be used to view the news item, such as smartphones, tablets, computers, and TVs.

ACIC. A causal inference data analysis challenge has been held every year at the Atlantic Causal Inference Conference since 2016, which presents different data sets for a variety of causal inference problems. Below we describe in detail two typical datasets, ACIC2016 and ACIC2018. A summary of the latest conference dataset about ACIC can be found in [159].

The ACIC 2016 consists of 77 datasets with different degrees of nonlinearity, sparsity, correlation between treatment assignment and outcome, and overlap between treatment effects. Covariates are derived from real data from the IHDP[104] dataset, which consists of 58 variables and 4802 samples[160]. The simulation model generates treatment, factual and counterfactual outcomes, while the selection bias is created by removing treated children who are mothers of nonwhites. The ACIC 2018 is a benchmarking dataset for causal inference that is commonly used[161]. It is a semi-synthetic dataset about infant births and deaths[162] and contains 63 datasets with each drawn randomly from a different distribution, which are then generated by a simulation process.

TCGA. As the world's largest and most comprehensive genomic database, the Cancer Genome Atlas (TCGA)[109] contains billions of genomes. A total of 9658 individuals are included in the TCGA[109] dataset, the treatment regimens are drug treatment, chemotherapy, and surgery, and the outcome is the risk of developing cancer after treatment.

PK-PD model of tumor growth. A model of pharmacokinetic-pharmacodynamics (PK-PD)[163] can be used to explore dose-response relationships and suggest optimal treatments. Among its key functions are the combination of chemotherapy and radiotherapy effects, post-treatment cellular regeneration, patient death or recovery, and cancer-based different gaze distributions of tumor size at the diagnostic stage, which make this model an excellent one for treating non-small cell lung cancer patients. The PKPD model enables clinicians to explore hypotheses about dose-response relationships and suggest optimal treatment options[164, 165]. In the most classic example of PK-PD, tumor growth[163] with time-dependent confounding can be predicted by observing the expected response to treatment, chemotherapy, and radiotherapy.

MIMIC III. Medical Information Mart for Intensive Care(MIMIC III)[166] is a database of electronic health records from ICU patients. The benchmark dataset consists of 7413 samples with 25 covariates after filtering for missing values. As far as treatment options go, antibiotics, vasopressors, and mechanical ventilators are the most common options in the ICU to treat patients with sepsis. A number of laboratory use patient vital signs over time as a measure to assess the effects of antibiotics, vasopressors, and mechanical ventilators on the following covariates, including white blood cells, blood pressure, and oxygen saturation. A comprehensive and detailed description of the clinical data can be found in [167].

NICO. There is a bias in sample selection when using the image dataset NICO with context for object classification[125]. Cat or dog classification in the "animals" dataset in NICO is seen as a benchmark distribution for non-i.i.d[168]. The parameters include the time of sampling, whether to sample, the context, and the semantic shape of cats and dogs, as well as the "grass" and "snow" environment.

CMNIST. A dataset of handwriting recognition with confusion bias(CMNIST) is based on MNIST[169] and labels the digits 0 to 4 and 5-9 to two outputs, namely green and red. The therapeutic input derived from color-evoked stimulus-related intensity parameters. Among covariates are number and color painting times, and whether or not to paint.

ADNI. Alzheimer's Disease Neuroimaging Initiative(ADNI)[170] dataset has three latent representation outputs Alzheimer's Disease, Mild Cognitive Impairment and Normal Control. The covariates are age and TAU[171], which determine whether Magnetic resonance imaging should be used as an input for therapy.

| Datasets | Binary | Multiple | Continuous dose | Times series | Structured |
|--------------|--------|----------|-----------------|--------------|------------|
| IHDP | ✓ | ✓ | × | × | × |
| Jobs | ✓ | × | × | × | × |
| Twins | ✓ | × | × | × | × |
| News | ✓ | ✓ | ✓ | × | × |
| ACIC | × | ✓ | ✓ | × | × |
| TCGA | × | × | ✓ | × | ✓ |
| Tumor Growth | × | × | × | ✓ | × |
| MIMIC III | × | × | ✓ | × | × |
| NICO | ✓ | × | × | × | × |
| CMNIST | ✓ | × | × | × | × |
| ADNI | × | ✓ | × | × | × |
| COVID-19 | × | ✓ | × | × | × |
| CPRD | × | × | × | ✓ | × |
| BlogCatalog | × | ✓ | × | × | ✓ |
| Flickr | × | ✓ | × | × | ✓ |

Table 3: Overview of some open available datasets for causal analysis and their application scenario

COVID-19. During the first peak of the pandemic, dataset COVID-19[107, 106] Hospitalization in England Surveillance System (CHESS) collected individual-level risk factors, treatments, and outcomes from 3090 ICU patients. There are a number of covariates, including factors such as age and multiple morbidity, as well as treatment parameters, such as ventilation and antiviral drugs. The outcome is the length of stay in the intensive care unit[172].

CPRD. Clinical Practice Research Datalink (CPRD) contains records from NHS general practice clinics in the United Kingdom, covering approximately 6.9 percent of the country’s population[173]. National mortality records and hospital event statistics indicate that CPRD is associated with secondary care admissions. Low-density lipoprotein is measured after CPRD is initiated, and treatment is defined as the date of first prescription. As temporal covariates, the following risk factors is measured before treatment initiation: high-density lipoprotein cholesterol, blood pressure, pulse, creatinine, triglycerides, and smoking status. HPS registry participants are selected from 125,784 individuals who meet the eligibility criteria. A total of 17,371 treatment groups and 24,557 control groups are divided into three equally sized subsets for training, validation, and testing.

BlogCatalog. BlogCatalog is an online community where users post blogs. In the dataset, each instance is a blogger[174]. Each edge represents a social relationship between two bloggers. Blog descriptions contain keywords represented as a bag-of-words. Blog reader opinions as input, whether blog-created content gets more comments on mobile or desktop as therapy, parameters for individual treatment effect estimation are derived from the content of readers’ comments on mobile (than desktop). The blogger belongs to the treatment group if people reads more on a mobile device than on a desktop device, and vice versa.

Flickr. Flickr is an online social networking site where users can share photos and videos[175]. The dataset consists of instances representing users, and edges representing social relationships between them. Tags of interest are represented by the features of each user. Generally, Settings and assumptions are the same as for BlogCatalog dataset.

| Datasets | Links | Methods |
|--------------|--|---|
| IHDP | https://www.fredjio.com/files | [40, 110, 42, 53, 19, 112, 44, 43, 41, 33, 70, 54, 116, 55, 118, 123, 124, 57, 129, 69, 131, 147, 129, 77, 152] |
| Jobs | http://users.nber.org/rdebejia/data/newdata2.html | [42, 53, 44, 43, 54, 55, 123, 129, 130, 76, 152, 151] |
| Twins | www.nber.org/data/linked-birth-infant-death-data-vital-statistics-data.html | [53, 44, 72, 43, 54, 55, 119, 123, 129, 130] |
| News | https://archive.ics.uci.edu/ml/datasets/bag+of+words | [40, 41, 33, 120, 73, 76, 56, 57, 77, 151] |
| ACIC | https://www.synapse.org/ACIC2018Challenge | [70, 131, 123, 176, 177, 178, 179, 180, 181, 182, 133] |
| TCGA | https://gdc.cancer.gov/ | [120, 73, 76, 77, 156, 183, 184, 185, 186, 187] |
| Tumor Growth | www.nature.com/scientificreports/ | [75, 121, 188, 189, 190, 191] |
| MIMIC III | https://mimic.physionet.org/ | [122, 123, 73, 56, 76, 192] |
| NICO | https://www.dropbox.com/sh/8mouawi5guaupyb/AAD4fdySrA6fn3PgShhKwFgvad1=0 | [125, 193, 194, 195, 196, 197] |
| CMNIST | https://trends.google.com/trends/explore?date=all&q=mnist | [125, 198, 74, 199, 200, 201, 202, 203, 204] |
| ADNI | www.loni.ucla.edu/ADNI | [125, 205, 206, 207, 208] |
| COVID-19 | https://www.heyvhale.com/mw/dataset/5e8ee81fe7ec38002d00f9cb | [132, 209, 210, 211] |
| CPRD | https://academic.oup.com/ije/article/44/3/827/632531 | [101, 212, 213, 214, 215, 216, 217] |
| BlogCatalog | https://www.blogcatalog.com/ | [102, 218, 219] |
| Flickr | https://www.flickr.com | [102] |

Table 4: The web links to the open available datasets and the related models that have used them for performance evaluation

6.2 Source codes

In addition to the popularly used datasets as motioned above, we also list in Table 5 the available source codes for some representative models and the relevant dataset they have used.

| Methods | Datasets | Framework | Links |
|------------------------------|--------------------------------|-------------|---|
| DCN-PD[110] | IHDP | Pytorch | https://github.com/Shantanu48114860/Deep-Counterfactual-Networks-with-Propensity-Dropout |
| BNN[40],CFRNet[42] | IHDP,Jobs,News | Tensorflow | https://github.com/clinicalml/cfrnet |
| CEVAE[53] | IHDP,Twins,Jobs | Tensorflow | https://github.com/AMLab-Amsterdam/CEVAE |
| GANITE[44] | IHDP,Twins,Jobs | Tensorflow | https://github.com/jayoon0823/GANITE |
| SITE[43] | IHDP,Twins,Jobs | Tensorflow | https://github.com/Usier-Yi/SITE |
| R-MSN[75] | PK-PD model of tumor growth | Tensorflow | https://github.com/sjblin/rman_nips_2018 |
| PM[41] | IHDP,News | Tensorflow | https://github.com/d916b/perfect_match |
| Dragonnet[70] | IHDP,ACIC | Tensorflow | https://github.com/clauidiashi57/dragonnet |
| DKLITE[55] | IHDP,Twins,Jobs | Tensorflow | https://github.com/vanderschaarlab/mlforhealthlabpub/tree/main/alg/dklite |
| CRN[121] | PK-PD model of tumor growth | Tensorflow | https://github.com/vanderschaarlab/mlforhealthlabpub/tree/main/alg/counterfactual_recurrent_network |
| TSJ[122] | MIMIC III | Tensorflow | https://github.com/vanderschaarlab/mlforhealthlabpub/tree/main/alg/time_series_deconfounder |
| ABCEI[123] | IHDP,Twins,Jobs,ACIC,MIMIC III | Tensorflow | https://github.com/octeuer/Adversarial-Balancing-based-representation-learning-for-Causal-Effect-Inference |
| LaCIM[125] | NICO,CMNIST,ADNI | Pytorch | https://github.com/wubotong/LaCIM |
| SCIGAN[73] | TCGA,News,MIMIC III | Tensorflow | https://github.com/loanabica/SCIGAN |
| DRNet[56] | TCGA,News,MIMIC III | Tensorflow | https://github.com/d909b/drnet |
| VCNet[57] | IHDP,News | Pytorch | https://github.com/lushleaf/varying-coefficient-net-with-functional-tr |
| DeR-CFR[69] | IHDP | Tensorflow | https://github.com/anpww/DeR-CFR |
| DONUT[130] | IHDP,Twins,Jobs | Tensorflow | https://github.com/tohhatt/donut |
| FlexTENet[131],CATENets[147] | IHDP,Twins,ACIC | Jax,Pytorch | https://github.com/AliciaCuthr/CATEMets |
| SCP[132] | COVID-19 | Pytorch | https://github.com/vanderschaarlab/Single-Cause-Perturbation-NeurIPS-2021 |
| SyncTwin[101] | CPRD | Pytorch | https://github.com/vanderschaarlab/SyncTwin-NeurIPS-2021 |
| TransTEE[77] | IHDP,News,TCGA | Pytorch | https://github.com/hlzhang109/TransTEE |
| CF-CV[146] | IHDP | Tensorflow | https://github.com/usaito/counterfactual-cv |
| CGN[74] | MNIST,ImageNet | Pytorch | https://github.com/autonomousvision/counterfactual_generative_networks |
| DESCN[133] | ACIC,EpiSpsy | Pytorch | https://github.com/kailiang-zhong/DESCN |

Table 5: Overview of some available datasets and web links to them

By combining related methods, datasets, and source codes, we can more easily identify the innovation points in each model. Meanwhile, it will also facilitate more fair comparison in performance evaluation. In addition, undoubtedly, these source codes will also greatly promote the development of research community about causal inference. As an example, the covariate decomposition is applied to the Dragonnet[70] model when combined with the DeR-CFR[69] model to make a further model optimization. By applying the TransTEE[77] attention mechanism to the representation balance part of VCNet[57] or DRNet[56], the continuous dose estimation curve can be fitted more accurately. It also means the latest advances in causal analysis have also benefited from or inspired by some previous representative works.

6.3 Experiment

We also provide an experimental summary of the binary treatment, multiple treatment and continuous-dose treatment scenarios on the above datasets, respectively. it should be pointed out that the reported results are under unified dataset setting for the compared models. Detailed experimental results and performance comparisons can be found in Tables 6, 7, 8 and 9, respectively, in which the **Mean \pm Std** of the estimated treatment effect results (lower better) are presented.

6.3.1 Settings and results for multiple and continue-dose treatment

In multiple and continuous dose treatment situations, there are three public datasets including TCGA[109], News[40] and MIMIC III[166] that are derived from[56, 73]. The datasets are split into 64/16/20% for training, validation, and testing respectively. The experimental results of TARNet[42], TransTEE[77] and VCNet[57] on the TCGA dataset in Table 6 are derived from the re-implementation of the source code.

Three treatments are used in the experiment[120, 73], each with a dose. In addition, each treatment, w , is associated with a set of parameters, $\mathbf{v}_1^w, \mathbf{v}_2^w, \mathbf{v}_3^w$. These parameters are sampled randomly by sampling a vector from $\mathcal{N}(\mathbf{0}, \mathbf{I})$ and then normalized. The experiments add $\epsilon \sim \mathcal{N}(0, 0.2)$ noise to the results. Interventions are assigned by drawing a dose d_w from the beta distribution for each treatment, $d_w | \mathbf{x} \sim \text{Beta}(\alpha, \beta_w)$. After that, the experiment assigns a treatment based on $w_f | \mathbf{x} \sim \text{Categorical}(\text{softmax}(\kappa f(\mathbf{x}, d_w)))$ where increasing κ increases the selection bias.

TCGA: This version uses the measurements of the 4000 most variable genes. Each feature of the gene expression data is scaled in the $[0, 1]$ interval. The experiment gives meaning to the treatment and dose by considering the treatment as chemotherapy/radiotherapy/immunotherapy and its corresponding dose[56].

News: The experiments intercepted 10,000 news articles, each with 2,858 features. Treatment and dose are given meaning, with treatment referring to the viewing device used to read the article (e.g., phone, tablet, etc.) and dose referring to the amount of time spent reading the article[42, 56].

MIMIC: The experiments intercepted 3000 patients that receive antibiotics treatment, using 9 clinical covariates, namely age, temperature, heart rate, systolic and diastolic blood pressure, SpO2, FiO2, glucose, and white blood cell

count, measured at start of ICU stay. Likewise, the features is scaled in the $[0, 1]$ interval. Different antibiotics and their corresponding doses are considered as treatment[73].

| Methods | TCGA | | | News | | | MIMIC | | |
|------------------|-----------------|-----------------|-----------------|-----------------|-----------------|-----------------|-----------------|-----------------|-----------------|
| | MISE | DPE | PE | MISE | DPE | PE | MISE | DPE | PE |
| TARNet[42] | 5.76 \pm 0.15 | 0.53 \pm 0.06 | 0.65 \pm 0.07 | — | — | — | — | — | — |
| DRN-W[56] | 3.71 \pm 0.12 | 0.50 \pm 0.05 | 0.63 \pm 0.05 | 5.07 \pm 0.12 | 4.21 \pm 0.11 | 4.56 \pm 0.12 | 4.47 \pm 0.12 | 0.53 \pm 0.05 | 1.37 \pm 0.05 |
| DRNet[56] | 3.64 \pm 0.12 | 0.51 \pm 0.05 | 0.67 \pm 0.05 | 4.98 \pm 0.12 | 4.39 \pm 0.11 | 4.17 \pm 0.11 | 4.45 \pm 0.12 | 0.52 \pm 0.05 | 1.44 \pm 0.05 |
| DRGAN,SCIGAN[73] | 1.89 \pm 0.05 | 0.31 \pm 0.05 | 0.25 \pm 0.05 | 3.71 \pm 0.05 | 4.14 \pm 0.11 | 3.90 \pm 0.05 | 2.09 \pm 0.12 | 0.51 \pm 0.05 | 0.32 \pm 0.05 |
| VCNet[57] | 6.36 \pm 0.11 | 0.22 \pm 0.04 | 0.32 \pm 0.02 | — | — | — | — | — | — |
| TransTEE[77] | 6.40 \pm 0.14 | 0.17 \pm 0.03 | 0.78 \pm 0.05 | — | — | — | — | — | — |
| TransTEE+TR[77] | 6.26 \pm 0.13 | 0.08 \pm 0.02 | 0.96 \pm 0.06 | — | — | — | — | — | — |
| TransTEE+PTR[77] | 6.36 \pm 0.14 | 0.18 \pm 0.03 | 0.81 \pm 0.05 | — | — | — | — | — | — |

Table 6: Overview of performance comparisons on TCGA, News, and MIMIC datasets by some representative models in the case of multiple and continue-dose treatments

6.3.2 Settings and results for binary treatment

In binary treatment situation, the datasets are the same as[42, 43, 54], which are three public datasets, i.e., IHDP[104], Jobs[91], and Twins[158]. On IHDP and Twins datasets, the average over 10 realizations with 63/27/10 ratio of train/validation/test splits, and on Jobs dataset, the average over 10 train/validation/test splits with ratios 56/24/20. Relevant experimental results can be found in Tables 7, 8 and 9.

IHDP: The treatment group is made unbalanced by removing a subset of the biased treatment population prior to the experiment. The simulated results adopt the setting "A" of the NPCI[220] package. As with[157], the real effect is calculated using noise-free results. Moreover, by constructing a biased subsample of the IHDP dataset the impact of the growing imbalance between the original treatment groups can be studied.

Twins: This version focuses on same-sex twin couples weighing less than 2,000 grams. After eliminating the records containing missing features, the final dataset contains 5409 records. The procedure $T_i | \mathbf{x}_i \sim \text{Bern}(\text{Sigmoid}(\mathbf{w}^T \mathbf{x} + n))$, where $\mathbf{w}^T \sim \mathcal{U}((-0.1, 0.1)^{40 \times 1})$ and $n \sim \mathcal{N}(0, 0.1)$ is used in the experiments to selectively choose one of the twins as an observation and hide the other one, generating a selection bias. The average over 10 realizations with 63/27/10 ratio of train/validation/test splits.

Jobs: Jobs is a binary classification task, in which the goal is to use the feature set of[221] to predict unemployment. The LaLonde trial sample[222] consists of 297 treatments and 425 controls, and the PSID comparison groups contains 2490 controls. At the end of study, a total of 482 (15%) subjects are unemployed.

| Methods | IHDP(ϵ_{ATE}) | | IHDP(ϵ_{PEHE}) | |
|--------------------------|--------------------------|-------------------|---------------------------|-------------------|
| | In-sample | Out-sample | In-sample | Out-sample |
| BNN[40, 42] | 0.37 \pm 0.03 | 0.42 \pm 0.03 | 2.2 \pm 0.1 | 2.1 \pm 0.1 |
| TARNet[42] | 0.26 \pm 0.01 | 0.28 \pm 0.01 | 0.88 \pm 0.02 | 0.95 \pm 0.02 |
| CFR _{MMD} [42] | 0.30 \pm 0.01 | 0.31 \pm 0.01 | 0.73 \pm 0.01 | 0.78 \pm 0.02 |
| CFR _{WASS} [42] | 0.25 \pm 0.01 | 0.27 \pm 0.01 | 0.71 \pm 0.02 | 0.76 \pm 0.02 |
| CEVAE[53] | 0.34 \pm 0.01 | 0.46 \pm 0.02 | 2.7 \pm 0.1 | 2.6 \pm 0.1 |
| GANITE[44] | 0.43 \pm 0.05 | 0.49 \pm 0.05 | 1.9 \pm 0.4 | 2.4 \pm 0.4 |
| SITE[43] | — | — | 0.604 \pm 0.093 | 0.656 \pm 0.108 |
| ACE[54] | — | — | 0.489 \pm 0.046 | 0.541 \pm 0.061 |
| DKLITE[55] | — | — | 0.52 \pm 0.02 | 0.65 \pm 0.03 |
| DR-CFR[118] | 0.240 \pm 0.032 | 0.261 \pm 0.036 | 0.657 \pm 0.028 | 0.789 \pm 0.091 |
| CETransformer[129] | — | — | 0.46 \pm 0.02 | 0.51 \pm 0.03 |
| DeR-CFR[69] | 0.130 \pm 0.020 | 0.147 \pm 0.022 | 0.444 \pm 0.020 | 0.529 \pm 0.068 |
| DONUT[130] | 0.13 \pm 0.01 | 0.19 \pm 0.02 | — | — |

Table 7: Overview of performance comparisons on IHDP dataset by some representative models in the case of binary treatment

| Methods | Twins($\hat{\epsilon}_{ATE}$) | | Twins(ϵ_{PEHE}) | |
|--|---------------------------------|---------------------|----------------------------|-------------------|
| | In-sample | Out-sample | In-sample | Out-sample |
| BNN[40, 42] | 0.0056 ± 0.0032 | 0.0203 ± 0.0071 | 0.307 ± 0.001 | 0.309 ± 0.004 |
| TARNet[42] | 0.0108 ± 0.0017 | 0.0151 ± 0.0018 | 0.314 ± 0.001 | 0.313 ± 0.002 |
| CFR _{MMD} [42] | — | — | 0.312 ± 0.001 | 0.316 ± 0.003 |
| CFR _{WASS} [42] 0.0112 ± 0.0016 | 0.0284 ± 0.0032 | 0.308 ± 0.001 | 0.309 ± 0.003 | — |
| GANITE[44] | 0.0058 ± 0.0017 | 0.0089 ± 0.0075 | — | — |
| SITE[43] | — | — | 0.309 ± 0.002 | 0.311 ± 0.004 |
| ACE[54] | — | — | 0.306 ± 0.000 | 0.301 ± 0.002 |
| DKLITE[55] | — | — | 0.288 ± 0.001 | 0.293 ± 0.003 |
| CETransformer[129] | — | — | 0.287 ± 0.001 | 0.289 ± 0.002 |
| DONUT[130] | 0.0025 ± 0.0016 | 0.0033 ± 0.0026 | — | — |

Table 8: **Overview of performance comparisons on Twins dataset by some representative models in the case of binary treatment**

| Methods | Jobs(ϵ_{ATT}) | | Jobs($\mathcal{R}_{pol}(\pi_f)$) | |
|--------------------------|--------------------------|-----------------|------------------------------------|-------------------|
| | In-sample | Out-sample | In-sample | Out-sample |
| BNN[40, 42] | 0.04 ± 0.01 | 0.09 ± 0.04 | 0.20 ± 0.01 | 0.24 ± 0.02 |
| TARNet[42] | 0.05 ± 0.02 | 0.11 ± 0.04 | 0.17 ± 0.01 | 0.21 ± 0.01 |
| CFR _{MMD} [42] | 0.04 ± 0.01 | 0.08 ± 0.03 | 0.18 ± 0.00 | 0.21 ± 0.01 |
| CFR _{WASS} [42] | 0.04 ± 0.01 | 0.09 ± 0.03 | 0.17 ± 0.01 | 0.21 ± 0.01 |
| CEVAE[53] | 0.02 ± 0.01 | 0.03 ± 0.01 | 0.15 ± 0.00 | 0.26 ± 0.00 |
| GANITE[44] | 0.01 ± 0.01 | 0.06 ± 0.03 | 0.13 ± 0.01 | 0.14 ± 0.01 |
| SITE[43] | — | — | 0.224 ± 0.004 | 0.219 ± 0.009 |
| ACE[54] | — | — | 0.216 ± 0.005 | 0.215 ± 0.009 |
| DKLITE[55] | — | — | 0.13 ± 0.01 | 0.14 ± 0.01 |
| CETransformer[129] | — | — | 0.12 ± 0.01 | 0.13 ± 0.00 |
| DONUT[130] | 0.01 ± 0.00 | 0.06 ± 0.05 | — | — |
| SCI[76] | — | — | 0.204 ± 0.008 | 0.225 ± 0.014 |

Table 9: **Overview of performance comparisons on Jobs dataset by some representative models in the case of binary treatment**

7 Conclusions

Deep causal models have become increasingly popular as a research topic because of the development of causal inference and deep learning. It is possible to improve causal effect estimation accuracy and unbiasedness by applying deep network models to causal inference. Moreover, the deep network can be optimized and improved by the profound theory used in causal inference. This survey presents the development of deep causal models and the evolution of various methods. Firstly, the basic knowledge related to the field of causal inference is adhibited. Then, we present the classical treatments and metrics. Additionally, we provide a comprehensive analysis of the deep causal model from temporal development. Next, we divide the deep causal modeling methods into five groups with an overview and analysis. Furthermore, We furnish a comprehensive conclusion of the application of causal inference in industry. Finally, we summarize the relevant benchmark datasets, open source codes, and performance results as experimental guidelines.

Since 2016, causal inference has been combined with deep learning models for the first time in the binary treatment case for estimation of counterfactual outcomes. So far, deep causal models have been used for time-series, multivariate treatment, and continuous-dose treatment situations. It is inseparable from the proposal of deep network models such as AE, GAN, RNN, and Transformer by researchers in the field of deep learning, the generation and simulation of datasets such as IHDP, Twins, Jobs, News, and TCGA by researchers in the field of statistics, and the exploration of ATE, PEHE, MISE, DPE by researchers in industry guided with the theory of potential outcome framework. We believe that with the joint efforts of everyone in the community of causal learning, deep causal models will flourish for the benefit of society

and humanity. Summary material for this survey can be found at https://github.com/alwaysmodest/A_Survey_of_Deep_Causal_Models.

References

- [1] Ruocheng Guo, Lu Cheng, Jundong Li, P Richard Hahn, and Huan Liu. A survey of learning causality with data: Problems and methods. *ACM Computing Surveys (CSUR)*, 53(4):1–37, 2020.
- [2] Liuyi Yao, Zhixuan Chu, Sheng Li, Yaliang Li, Jing Gao, and Aidong Zhang. A survey on causal inference. *ACM Transactions on Knowledge Discovery from Data (TKDD)*, 15(5):1–46, 2021.
- [3] Wei Sun, Pengyuan Wang, Dawei Yin, Jian Yang, and Yi Chang. Causal inference via sparse additive models with application to online advertising. In *Twenty-Ninth AAAI Conference on Artificial Intelligence*, 2015.
- [4] Pengyuan Wang, Wei Sun, Dawei Yin, Jian Yang, and Yi Chang. Robust tree-based causal inference for complex ad effectiveness analysis. In *Proceedings of the Eighth ACM International Conference on Web Search and Data Mining*, pages 67–76, 2015.
- [5] Sheng Li, Nikos Vlassis, Jaya Kawale, and Yun Fu. Matching via dimensionality reduction for estimation of treatment effects in digital marketing campaigns. In *IJCAI*, pages 3768–3774, 2016.
- [6] Christian Fong, Chad Hazlett, and Kosuke Imai. Covariate balancing propensity score for a continuous treatment: Application to the efficacy of political advertisements. *The Annals of Applied Statistics*, 12(1):156–177, 2018.
- [7] Nir Rosenfeld, Yishay Mansour, and Elad Yom-Tov. Predicting counterfactuals from large historical data and small randomized trials. In *Proceedings of the 26th International Conference on World Wide Web Companion*, pages 602–609, 2017.
- [8] Bowen Yuan, Jui-Yang Hsia, Meng-Yuan Yang, Hong Zhu, Chih-Yao Chang, Zhenhua Dong, and Chih-Jen Lin. Improving ad click prediction by considering non-displayed events. In *Proceedings of the 28th ACM International Conference on Information and Knowledge Management*, pages 329–338, 2019.
- [9] Miroslav Dudík, John Langford, and Lihong Li. Doubly robust policy evaluation and learning. *arXiv preprint arXiv:1103.4601*, 2011.
- [10] Akos Lada, Alexander Peysakhovich, Diego Aparicio, and Michael Bailey. Observational data for heterogeneous treatment effects with application to recommender systems. In *Proceedings of the 2019 ACM Conference on Economics and Computation*, pages 199–213, 2019.
- [11] Tobias Schnabel, Adith Swaminathan, Ashudeep Singh, Navin Chandak, and Thorsten Joachims. Recommendations as treatments: Debiasing learning and evaluation. In *international conference on machine learning*, pages 1670–1679. PMLR, 2016.
- [12] Yuta Saito. Eliminating bias in recommender systems via pseudo-labeling. *arXiv preprint arXiv:1910.01444*, 2019.
- [13] Adith Swaminathan, Akshay Krishnamurthy, Alekh Agarwal, Miro Dudik, John Langford, Damien Jose, and Imed Zitouni. Off-policy evaluation for slate recommendation. *Advances in Neural Information Processing Systems*, 30, 2017.
- [14] Wenhao Zhang, Wentian Bao, Xiao-Yang Liu, Keping Yang, Quan Lin, Hong Wen, and Ramin Ramezani. A causal perspective to unbiased conversion rate estimation on data missing not at random. *arXiv preprint arXiv:1910.09337*, 2019.
- [15] Stephen Bonner and Flavian Vasile. Causal embeddings for recommendation. In *Proceedings of the 12th ACM conference on recommender systems*, pages 104–112, 2018.
- [16] Xiaojie Wang, Rui Zhang, Yu Sun, and Jianzhong Qi. Doubly robust joint learning for recommendation on data missing not at random. In *International Conference on Machine Learning*, pages 6638–6647. PMLR, 2019.
- [17] Uri Shalit. Can we learn individual-level treatment policies from clinical data? *Biostatistics*, 21(2):359–362, 2020.
- [18] Ronald C Kessler, Robert M Bossarte, Alex Luedtke, Alan M Zaslavsky, and Jose R Zubizarreta. Machine learning methods for developing precision treatment rules with observational data. *Behaviour Research and Therapy*, 120:103412, 2019.
- [19] Onur Atan, James Jordon, and Mihaela Van der Schaar. Deep-treat: Learning optimal personalized treatments from observational data using neural networks. In *Proceedings of the AAAI Conference on Artificial Intelligence*, volume 32, 2018.

- [20] Doina Precup. Eligibility traces for off-policy policy evaluation. *Computer Science Department Faculty Publication Series*, page 80, 2000.
- [21] Onur Atan, William R Zame, and Mihaela van der Schaar. Learning optimal policies from observational data. *arXiv preprint arXiv:1802.08679*, 2018.
- [22] Nathan Kallus and Masatoshi Uehara. Intrinsically efficient, stable, and bounded off-policy evaluation for reinforcement learning. *Advances in neural information processing systems*, 32, 2019.
- [23] Lihong Li, Wei Chu, John Langford, Taesup Moon, and Xuanhui Wang. An unbiased offline evaluation of contextual bandit algorithms with generalized linear models. In *Proceedings of the Workshop on On-line Trading of Exploration and Exploitation 2*, pages 19–36. JMLR Workshop and Conference Proceedings, 2012.
- [24] Adith Swaminathan and Thorsten Joachims. Counterfactual risk minimization: Learning from logged bandit feedback. In *International Conference on Machine Learning*, pages 814–823. PMLR, 2015.
- [25] Guy Tennenholtz, Uri Shalit, and Shie Mannor. Off-policy evaluation in partially observable environments. In *Proceedings of the AAAI Conference on Artificial Intelligence*, volume 34, pages 10276–10283, 2020.
- [26] Hao Zou, Kun Kuang, Boqi Chen, Peixuan Chen, and Peng Cui. Focused context balancing for robust offline policy evaluation. In *Proceedings of the 25th ACM SIGKDD International Conference on Knowledge Discovery & Data Mining*, pages 696–704, 2019.
- [27] Nathan Kallus and Angela Zhou. Confounding-robust policy improvement. *Advances in neural information processing systems*, 31, 2018.
- [28] Reid Pryzant, Kelly Shen, Dan Jurafsky, and Stefan Wagner. Deconfounded lexicon induction for interpretable social science. In *Proceedings of the 2018 Conference of the North American Chapter of the Association for Computational Linguistics: Human Language Technologies, Volume 1 (Long Papers)*, pages 1615–1625, 2018.
- [29] Naoki Egami, Christian J Fong, Justin Grimmer, Margaret E Roberts, and Brandon M Stewart. How to make causal inferences using texts. *arXiv preprint arXiv:1802.02163*, 2018.
- [30] Chenhao Tan, Lillian Lee, and Bo Pang. The effect of wording on message propagation: Topic-and author-controlled natural experiments on twitter. *arXiv preprint arXiv:1405.1438*, 2014.
- [31] Zach Wood-Doughty, Ilya Shpitser, and Mark Dredze. Challenges of using text classifiers for causal inference. In *Proceedings of the Conference on Empirical Methods in Natural Language Processing. Conference on Empirical Methods in Natural Language Processing*, volume 2018, page 4586. NIH Public Access, 2018.
- [32] Katherine A Keith, David Jensen, and Brendan O’Connor. Text and causal inference: A review of using text to remove confounding from causal estimates. *arXiv preprint arXiv:2005.00649*, 2020.
- [33] Liuyi Yao, Sheng Li, Yaliang Li, Hongfei Xue, Jing Gao, and Aidong Zhang. On the estimation of treatment effect with text covariates. In *International Joint Conference on Artificial Intelligence*, 2019.
- [34] Yulei Niu, Kaihua Tang, Hanwang Zhang, Zhiwu Lu, Xian-Sheng Hua, and Ji-Rong Wen. Counterfactual vqa: A cause-effect look at language bias. In *Proceedings of the IEEE/CVF Conference on Computer Vision and Pattern Recognition*, pages 12700–12710, 2021.
- [35] Arijit Ray, Karan Sikka, Ajay Divakaran, Stefan Lee, and Giedrius Burachas. Sunny and dark outside?! improving answer consistency in vqa through entailed question generation. *arXiv preprint arXiv:1909.04696*, 2019.
- [36] Meet Shah, Xinlei Chen, Marcus Rohrbach, and Devi Parikh. Cycle-consistency for robust visual question answering. In *Proceedings of the IEEE/CVF Conference on Computer Vision and Pattern Recognition*, pages 6649–6658, 2019.
- [37] Vedika Agarwal, Rakshith Shetty, and Mario Fritz. Towards causal vqa: Revealing and reducing spurious correlations by invariant and covariant semantic editing. In *Proceedings of the IEEE/CVF Conference on Computer Vision and Pattern Recognition*, pages 9690–9698, 2020.
- [38] Tan Wang, Jianqiang Huang, Hanwang Zhang, and Qianru Sun. Visual commonsense representation learning via causal inference. In *Proceedings of the IEEE/CVF Conference on Computer Vision and Pattern Recognition Workshops*, pages 378–379, 2020.
- [39] Siyuan Zhao and Neil Heffernan. Estimating individual treatment effect from educational studies with residual counterfactual networks. *International Educational Data Mining Society*, 2017.
- [40] Fredrik Johansson, Uri Shalit, and David Sontag. Learning representations for counterfactual inference. In *International conference on machine learning*, pages 3020–3029. PMLR, 2016.

- [41] Patrick Schwab, Lorenz Linhardt, and Walter Karlen. Perfect match: A simple method for learning representations for counterfactual inference with neural networks. *arXiv preprint arXiv:1810.00656*, 2018.
- [42] Uri Shalit, Fredrik D Johansson, and David Sontag. Estimating individual treatment effect: generalization bounds and algorithms. In *International Conference on Machine Learning*, pages 3076–3085. PMLR, 2017.
- [43] Liuyi Yao, Sheng Li, Yaliang Li, Mengdi Huai, Jing Gao, and Aidong Zhang. Representation learning for treatment effect estimation from observational data. *Advances in Neural Information Processing Systems*, 31, 2018.
- [44] Jinsung Yoon, James Jordon, and Mihaela Van Der Schaar. Ganite: Estimation of individualized treatment effects using generative adversarial nets. In *International Conference on Learning Representations*, 2018.
- [45] Kun Kuang, Peng Cui, Susan Athey, Ruoxuan Xiong, and Bo Li. Stable prediction across unknown environments. In *proceedings of the 24th ACM SIGKDD international conference on knowledge discovery & data mining*, pages 1617–1626, 2018.
- [46] Mehdi Gheisari, Guojun Wang, and Md Zakirul Alam Bhuiyan. A survey on deep learning in big data. In *2017 IEEE international conference on computational science and engineering (CSE) and IEEE international conference on embedded and ubiquitous computing (EUC)*, volume 2, pages 173–180. IEEE, 2017.
- [47] Reinaldo Padilha França, Ana Carolina Borges Monteiro, Rangel Arthur, and Yuzo Iano. An overview of deep learning in big data, image, and signal processing in the modern digital age. *Trends in Deep Learning Methodologies*, pages 63–87, 2021.
- [48] Qingchen Zhang, Laurence T Yang, Zhikui Chen, and Peng Li. A survey on deep learning for big data. *Information Fusion*, 42:146–157, 2018.
- [49] Bilal Jan, Haleem Farman, Murad Khan, Muhammad Imran, Ihtesham Ul Islam, Awais Ahmad, Shaukat Ali, and Gwanggil Jeon. Deep learning in big data analytics: a comparative study. *Computers & Electrical Engineering*, 75:275–287, 2019.
- [50] Supriyo Chakraborty, Richard Tomsett, Ramya Raghavendra, Daniel Harborne, Moustafa Alzantot, Federico Cerutti, Mani Srivastava, Alun Preece, Simon Julier, Raghuvver M Rao, et al. Interpretability of deep learning models: A survey of results. In *2017 IEEE smartworld, ubiquitous intelligence & computing, advanced & trusted computed, scalable computing & communications, cloud & big data computing, Internet of people and smart city innovation (smartworld/SCALCOM/UIC/ATC/CBDcom/IOP/SCI)*, pages 1–6. IEEE, 2017.
- [51] Quan-shi Zhang and Song-Chun Zhu. Visual interpretability for deep learning: a survey. *Frontiers of Information Technology & Electronic Engineering*, 19(1):27–39, 2018.
- [52] Pantelis Linardatos, Vasilis Papastefanopoulos, and Sotiris Kotsiantis. Explainable ai: A review of machine learning interpretability methods. *Entropy*, 23(1):18, 2020.
- [53] Christos Louizos, Uri Shalit, Joris M Mooij, David Sontag, Richard Zemel, and Max Welling. Causal effect inference with deep latent-variable models. *Advances in neural information processing systems*, 30, 2017.
- [54] Liuyi Yao, Sheng Li, Yaliang Li, Mengdi Huai, Jing Gao, and Aidong Zhang. Ace: Adaptively similarity-preserved representation learning for individual treatment effect estimation. In *2019 IEEE International Conference on Data Mining (ICDM)*, pages 1432–1437. IEEE, 2019.
- [55] Yao Zhang, Alexis Bellot, and Mihaela Schaar. Learning overlapping representations for the estimation of individualized treatment effects. In *International Conference on Artificial Intelligence and Statistics*, pages 1005–1014. PMLR, 2020.
- [56] Patrick Schwab, Lorenz Linhardt, Stefan Bauer, Joachim M Buhmann, and Walter Karlen. Learning counterfactual representations for estimating individual dose-response curves. In *Proceedings of the AAAI Conference on Artificial Intelligence*, volume 34, pages 5612–5619, 2020.
- [57] Lizhen Nie, Mao Ye, Qiang Liu, and Dan Nicolae. Vcnet and functional targeted regularization for learning causal effects of continuous treatments. *arXiv preprint arXiv:2103.07861*, 2021.
- [58] Naomi Altman and Martin Krzywinski. Points of significance: Association, correlation and causation. *Nature methods*, 12(10), 2015.
- [59] Meike Nauta, Doina Bucur, and Christin Seifert. Causal discovery with attention-based convolutional neural networks. *Machine Learning and Knowledge Extraction*, 1(1):19, 2019.
- [60] Clark Glymour, Kun Zhang, and Peter Spirtes. Review of causal discovery methods based on graphical models. *Frontiers in genetics*, 10:524, 2019.
- [61] Matthew J Vowels, Necati Cihan Camgoz, and Richard Bowden. D’ya like dags? a survey on structure learning and causal discovery. *ACM Computing Surveys (CSUR)*, 2021.

- [62] Amar Bhide, Prakesh S Shah, and Ganesh Acharya. A simplified guide to randomized controlled trials. *Acta obstetricia et gynecologica Scandinavica*, 97(4):380–387, 2018.
- [63] Christine M Steeger, Pamela R Buckley, Fred C Pampel, Charleen J Gust, and Karl G Hill. Common methodological problems in randomized controlled trials of preventive interventions. *Prevention Science*, 22(8):1159–1172, 2021.
- [64] Stephen A Kutcher, James M Brophy, Hailey R Banack, Jay S Kaufman, and Michelle Samuel. Emulating a randomised controlled trial with observational data: an introduction to the target trial framework. *Canadian Journal of Cardiology*, 37(9):1365–1377, 2021.
- [65] Gemma Hammerton and Marcus R Munafò. Causal inference with observational data: the need for triangulation of evidence. *Psychological medicine*, 51(4):563–578, 2021.
- [66] Nick Pawlowski, Daniel Coelho de Castro, and Ben Glocker. Deep structural causal models for tractable counterfactual inference. *Advances in Neural Information Processing Systems*, 33:857–869, 2020.
- [67] Donald B Rubin. Causal inference using potential outcomes: Design, modeling, decisions. *Journal of the American Statistical Association*, 100(469):322–331, 2005.
- [68] Donald B Rubin. Estimating causal effects of treatments in randomized and nonrandomized studies. *Journal of educational Psychology*, 66(5):688, 1974.
- [69] Anpeng Wu, Kun Kuang, Junkun Yuan, Bo Li, Runze Wu, Qiang Zhu, Yueting Zhuang, and Fei Wu. Learning decomposed representation for counterfactual inference. *arXiv preprint arXiv:2006.07040*, 2020.
- [70] Claudia Shi, David Blei, and Victor Veitch. Adapting neural networks for the estimation of treatment effects. *Advances in neural information processing systems*, 32, 2019.
- [71] Hyemi Kim, Seungjae Shin, JoonHo Jang, Kyungwoo Song, Weonyoung Joo, Wanmo Kang, and Il-Chul Moon. Counterfactual fairness with disentangled causal effect variational autoencoder. In *Proceedings of the AAAI Conference on Artificial Intelligence*, volume 35, pages 8128–8136, 2021.
- [72] Changhee Lee, Nicholas Mastronarde, and Mihaela van der Schaar. Estimation of individual treatment effect in latent confounder models via adversarial learning. *arXiv preprint arXiv:1811.08943*, 2018.
- [73] Ioana Bica, James Jordon, and Mihaela van der Schaar. Estimating the effects of continuous-valued interventions using generative adversarial networks. *Advances in Neural Information Processing Systems*, 33:16434–16445, 2020.
- [74] Axel Sauer and Andreas Geiger. Counterfactual generative networks. *arXiv preprint arXiv:2101.06046*, 2021.
- [75] Bryan Lim. Forecasting treatment responses over time using recurrent marginal structural networks. *advances in neural information processing systems*, 31, 2018.
- [76] Liuyi Yao, Yaliang Li, Sheng Li, Mengdi Huai, Jing Gao, and Aidong Zhang. Sci: Subspace learning based counterfactual inference for individual treatment effect estimation. In *Proceedings of the 30th ACM International Conference on Information & Knowledge Management*, pages 3583–3587, 2021.
- [77] Yi-Fan Zhang, Hanlin Zhang, Zachary C Lipton, Li Erran Li, and Eric P Xing. Can transformers be strong treatment effect estimators? *arXiv preprint arXiv:2202.01336*, 2022.
- [78] Liangyu Zhu, Wenbin Lu, and Rui Song. Causal effect estimation and optimal dose suggestions in mobile health. In *International Conference on Machine Learning*, pages 11588–11598. PMLR, 2020.
- [79] Paul Muentener and Elizabeth Bonawitz. The development of causal reasoning. 2018.
- [80] Bernhard Schölkopf. Causality for machine learning. In *Probabilistic and Causal Inference: The Works of Judea Pearl*, pages 765–804. 2022.
- [81] Kun Kuang, Lian Li, Zhi Geng, Lei Xu, Kun Zhang, Beishui Liao, Huaxin Huang, Peng Ding, Wang Miao, and Zhichao Jiang. Causal inference. *Engineering*, 6(3):253–263, 2020.
- [82] Bernhard Schölkopf, Francesco Locatello, Stefan Bauer, Nan Rosemary Ke, Nal Kalchbrenner, Anirudh Goyal, and Yoshua Bengio. Toward causal representation learning. *Proceedings of the IEEE*, 109(5):612–634, 2021.
- [83] Pedro Sanchez, Jeremy P Voisey, Tian Xia, Hannah I Watson, Alison Q O’Neil, and Sotirios A Tsaftaris. Causal machine learning for healthcare and precision medicine. *Royal Society Open Science*, 9(8):220638, 2022.
- [84] Hang Chen, Keqing Du, Xinyu Yang, and Chenguang Li. A review and roadmap of deep learning causal discovery in different variable paradigms, 2022.
- [85] Chen Gao, Yu Zheng, Wenjie Wang, Fuli Feng, Xiangnan He, and Yong Li. Causal inference in recommender systems: A survey and future directions, 2022.

- [86] Jean Kaddour, Aengus Lynch, Qi Liu, Matt J Kusner, and Ricardo Silva. Causal machine learning: A survey and open problems. *arXiv preprint arXiv:2206.15475*, 2022.
- [87] Ahmed M Alaa and Mihaela van der Schaar. Bayesian inference of individualized treatment effects using multi-task gaussian processes. *arXiv preprint arXiv:1704.02801*, 2017.
- [88] Thomas A Glass, Steven N Goodman, Miguel A Hernán, and Jonathan M Samet. Causal inference in public health. *Annual review of public health*, 34:61–75, 2013.
- [89] Marc Höfler. Causal inference based on counterfactuals. *BMC medical research methodology*, 5(1):1–12, 2005.
- [90] Markus Gangl. Causal inference in sociological research. *Annual review of sociology*, 36:21–47, 2010.
- [91] Robert J LaLonde. Evaluating the econometric evaluations of training programs with experimental data. *The American economic review*, pages 604–620, 1986.
- [92] Jeffrey A Smith and Petra E Todd. Does matching overcome lalonde’s critique of nonexperimental estimators? university of western ontario und university of pennsylvania. Technical report, mimeo, 2002.
- [93] Alexis Hannart, J Pearl, FEL Otto, P Naveau, and M Ghil. Causal counterfactual theory for the attribution of weather and climate-related events. *Bulletin of the American Meteorological Society*, 97(1):99–110, 2016.
- [94] Victor Chernozhukov, Iván Fernández-Val, and Blaise Melly. Inference on counterfactual distributions. *Econometrica*, 81(6):2205–2268, 2013.
- [95] Kun Zhang, Mingming Gong, and Bernhard Schölkopf. Multi-source domain adaptation: A causal view. In *Twenty-ninth AAAI conference on artificial intelligence*, 2015.
- [96] Kun Kuang, Peng Cui, Bo Li, Meng Jiang, and Shiqiang Yang. Estimating treatment effect in the wild via differentiated confounder balancing. In *Proceedings of the 23rd ACM SIGKDD International Conference on Knowledge Discovery and Data Mining*, pages 265–274, 2017.
- [97] Matt J Kusner, Joshua R Loftus, Chris Russell, and Ricardo Silva. Counterfactual fairness. *arXiv preprint arXiv:1703.06856*, 2017.
- [98] Sheng Li and Yun Fu. Matching on balanced nonlinear representations for treatment effects estimation. In *NIPS*, 2017.
- [99] Guido W Imbens and Donald B Rubin. *Causal inference in statistics, social, and biomedical sciences*. Cambridge University Press, 2015.
- [100] Donna Döpp-Zemel and AB Johan Groeneveld. High-dose norepinephrine treatment: determinants of mortality and futility in critically ill patients. *American Journal of Critical Care*, 22(1):22–32, 2013.
- [101] Zhaozhi Qian, Yao Zhang, Ioana Bica, Angela Wood, and Mihaela van der Schaar. Synctwin: Treatment effect estimation with longitudinal outcomes. *Advances in Neural Information Processing Systems*, 34, 2021.
- [102] Ruocheng Guo, Jundong Li, and Huan Liu. Learning individual causal effects from networked observational data. In *Proceedings of the 13th International Conference on Web Search and Data Mining*, pages 232–240, 2020.
- [103] Rajeev H Dehejia and Sadek Wahba. Causal effects in nonexperimental studies: Reevaluating the evaluation of training programs. *Journal of the American statistical Association*, 94(448):1053–1062, 1999.
- [104] Jeanne Brooks-Gunn, Fong-ruey Liaw, and Pamela Kato Klebanov. Effects of early intervention on cognitive function of low birth weight preterm infants. *The Journal of pediatrics*, 120(3):350–359, 1992.
- [105] Shiv Kumar Saini, Sunny Dhamnani, Akil Arif Ibrahim, and Prithviraj Chavan. Multiple treatment effect estimation using deep generative model with task embedding. In *The World Wide Web Conference*, pages 1601–1611, 2019.
- [106] Zhaozhi Qian, Ahmed M Alaa, Mihaela van der Schaar, and Ari Ercole. Between-centre differences for covid-19 icu mortality from early data in england. *Intensive Care Medicine*, 46(9):1779–1780, 2020.
- [107] Nicolai Haase, Ronni Plovsing, Steffen Christensen, Lone Musaeus Poulsen, Anne Craveiro Brøchner, Bodil Steen Rasmussen, Marie Helleberg, Jens Ulrik Staehr Jensen, Lars Peter Kloster Andersen, Hanna Siegel, et al. Characteristics, interventions, and longer term outcomes of covid-19 icu patients in denmark—a nationwide, observational study. *Acta Anaesthesiologica Scandinavica*, 65(1):68–75, 2021.
- [108] Leonid Galtchouk and Victor Konev. On sequential least squares estimates of autoregressive parameters. *Sequential Analysis*, 24(4):335–364, 2005.
- [109] John N Weinstein, Eric A Collisson, Gordon B Mills, Kenna R Shaw, Brad A Ozenberger, Kyle Ellrott, Ilya Shmulevich, Chris Sander, and Joshua M Stuart. The cancer genome atlas pan-cancer analysis project. *Nature genetics*, 45(10):1113–1120, 2013.

- [110] Ahmed M Alaa, Michael Weisz, and Mihaela Van Der Schaar. Deep counterfactual networks with propensity-dropout. *arXiv preprint arXiv:1706.05966*, 2017.
- [111] Carl Doersch. Tutorial on variational autoencoders. *arXiv preprint arXiv:1606.05908*, 2016.
- [112] Fredrik D Johansson, Nathan Kallus, Uri Shalit, and David Sontag. Learning weighted representations for generalization across designs. *arXiv preprint arXiv:1802.08598*, 2018.
- [113] Ian Goodfellow, Jean Pouget-Abadie, Mehdi Mirza, Bing Xu, David Warde-Farley, Sherjil Ozair, Aaron Courville, and Yoshua Bengio. Generative adversarial nets. *Advances in neural information processing systems*, 27, 2014.
- [114] Negar Hassanpour and Russell Greiner. Counterfactual regression with importance sampling weights. In *IJCAI*, pages 5880–5887, 2019.
- [115] Larry R Medsker and LC Jain. Recurrent neural networks. *Design and Applications*, 5:64–67, 2001.
- [116] Zichen Zhang, Qingfeng Lan, Lei Ding, Yue Wang, Negar Hassanpour, and Russell Greiner. Reducing selection bias in counterfactual reasoning for individual treatment effects estimation. *arXiv preprint arXiv:1912.09040*, 2019.
- [117] Jacob Benesty, Jingdong Chen, Yiteng Huang, and Israel Cohen. Pearson correlation coefficient. In *Noise reduction in speech processing*, pages 1–4. Springer, 2009.
- [118] Negar Hassanpour and Russell Greiner. Learning disentangled representations for counterfactual regression. In *International Conference on Learning Representations*, 2019.
- [119] Yunzhe Li, Kun Kuang, Bo Li, Peng Cui, Jianrong Tao, Hongxia Yang, and Fei Wu. Continuous treatment effect estimation via generative adversarial de-confounding. In *Proceedings of the 2020 KDD Workshop on Causal Discovery*, pages 4–22. PMLR, 2020.
- [120] Ioana Bica, James Jordon, and Mihaela van der Schaar. Individualised dose-response estimation using generative adversarial nets. *ICLR 2020 Conference Blind Submission*, 2019.
- [121] Ioana Bica, Ahmed M Alaa, James Jordon, and Mihaela van der Schaar. Estimating counterfactual treatment outcomes over time through adversarially balanced representations. *arXiv preprint arXiv:2002.04083*, 2020.
- [122] Ioana Bica, Ahmed Alaa, and Mihaela Van Der Schaar. Time series deconfounder: Estimating treatment effects over time in the presence of hidden confounders. In *International Conference on Machine Learning*, pages 884–895. PMLR, 2020.
- [123] Xin Du, Lei Sun, Wouter Duivesteijn, Alexander Nikolaev, and Mykola Pechenizkiy. Adversarial balancing-based representation learning for causal effect inference with observational data. *Data Mining and Knowledge Discovery*, 35(4):1713–1738, 2021.
- [124] Serge Assaad, Shuxi Zeng, Chenyang Tao, Shounak Datta, Nikhil Mehta, Ricardo Henao, Fan Li, and Lawrence Carin. Counterfactual representation learning with balancing weights. In *International Conference on Artificial Intelligence and Statistics*, pages 1972–1980. PMLR, 2021.
- [125] Xinwei Sun, Botong Wu, Xiangyu Zheng, Chang Liu, Wei Chen, Tao Qin, and Tie-yan Liu. Latent causal invariant model. *arXiv preprint arXiv:2011.02203*, 2020.
- [126] Hao Zou, Peng Cui, Bo Li, Zheyang Shen, Jianxin Ma, Hongxia Yang, and Yue He. Counterfactual prediction for bundle treatment. *Advances in Neural Information Processing Systems*, 33:19705–19715, 2020.
- [127] Sonali Parbhoo, Stefan Bauer, and Patrick Schwab. Ncore: Neural counterfactual representation learning for combinations of treatments. *arXiv preprint arXiv:2103.11175*, 2021.
- [128] Ashish Vaswani, Noam Shazeer, Niki Parmar, Jakob Uszkoreit, Llion Jones, Aidan N Gomez, Łukasz Kaiser, and Illia Polosukhin. Attention is all you need. *Advances in neural information processing systems*, 30, 2017.
- [129] Zhenyu Guo, Shuai Zheng, Zhizhe Liu, Kun Yan, and Zhenfeng Zhu. Cetransformer: Casual effect estimation via transformer based representation learning. In *Chinese Conference on Pattern Recognition and Computer Vision (PRCV)*, pages 524–535. Springer, 2021.
- [130] Tobias Hatt and Stefan Feuerriegel. Estimating average treatment effects via orthogonal regularization. In *Proceedings of the 30th ACM International Conference on Information & Knowledge Management*, pages 680–689, 2021.
- [131] Alicia Curth and Mihaela van der Schaar. On inductive biases for heterogeneous treatment effect estimation. *Advances in Neural Information Processing Systems*, 34, 2021.
- [132] Zhaozhi Qian, Alicia Curth, and Mihaela van der Schaar. Estimating multi-cause treatment effects via single-cause perturbation. *Advances in Neural Information Processing Systems*, 34, 2021.

- [133] Kailiang Zhong, Fengtong Xiao, Yan Ren, Yaorong Liang, Wenqing Yao, Xiaofeng Yang, and Ling Cen. Descn: Deep entire space cross networks for individual treatment effect estimation. In *Proceedings of the 28th ACM SIGKDD Conference on Knowledge Discovery and Data Mining*, pages 4612–4620, 2022.
- [134] Ruoqi Liu, Pin-Yu Chen, and Ping Zhang. Cure: A pre-training framework on large-scale patient data for treatment effect estimation. *medRxiv*, 2022.
- [135] Ruoqi Yu and Shulei Wang. Treatment effects estimation by uniform transformer. *arXiv preprint arXiv:2008.03738*, 2020.
- [136] Arthur Gretton, Karsten M Borgwardt, Malte J Rasch, Bernhard Schölkopf, and Alexander Smola. A kernel two-sample test. *The Journal of Machine Learning Research*, 13(1):723–773, 2012.
- [137] Cédric Villani. *Optimal transport: old and new*, volume 338. Springer, 2009.
- [138] Marco Cuturi and Arnaud Doucet. Fast computation of wasserstein barycenters. In *International conference on machine learning*, pages 685–693. PMLR, 2014.
- [139] Pierre Baldi and Peter J Sadowski. Understanding dropout. *Advances in neural information processing systems*, 26, 2013.
- [140] Paul R Rosenbaum. Propensity score. *Wiley Encyclopedia of Clinical Trials*, 2007.
- [141] Jeroen Berrevoets, James Jordon, Ioana Bica, Mihaela van der Schaar, et al. Organite: Optimal transplant donor organ offering using an individual treatment effect. *Advances in neural information processing systems*, 33:20037–20050, 2020.
- [142] Diederik P Kingma and Max Welling. Auto-encoding variational bayes. *arXiv preprint arXiv:1312.6114*, 2013.
- [143] Danilo Jimenez Rezende, Shakir Mohamed, and Daan Wierstra. Stochastic backpropagation and approximate inference in deep generative models. In *International conference on machine learning*, pages 1278–1286. PMLR, 2014.
- [144] Judea Pearl. The do-calculus revisited. *arXiv preprint arXiv:1210.4852*, 2012.
- [145] Jing Ma, Ruocheng Guo, Aidong Zhang, and Jundong Li. Multi-cause effect estimation with disentangled confounder representation. In *IJCAI*, pages 2790–2796, 2021.
- [146] Yuta Saito and Shota Yasui. Counterfactual cross-validation: Stable model selection procedure for causal inference models. In *International Conference on Machine Learning*, pages 8398–8407. PMLR, 2020.
- [147] Alicia Curth and Mihaela van der Schaar. Nonparametric estimation of heterogeneous treatment effects: From theory to learning algorithms. In *International Conference on Artificial Intelligence and Statistics*, pages 1810–1818. PMLR, 2021.
- [148] Raha Moraffah, Paras Sheth, Mansoor Karami, Anchit Bhattacharya, Qianru Wang, Anique Tahir, Adrienne Raglin, and Huan Liu. Causal inference for time series analysis: Problems, methods and evaluation. *Knowledge and Information Systems*, pages 1–45, 2021.
- [149] Sepp Hochreiter and Jürgen Schmidhuber. Long short-term memory. *Neural computation*, 9(8):1735–1780, 1997.
- [150] Ruoqi Liu, Changchang Yin, and Ping Zhang. Estimating individual treatment effects with time-varying confounders. In *2020 IEEE International Conference on Data Mining (ICDM)*, pages 382–391. IEEE, 2020.
- [151] Zhixuan Chu, Stephen L Rathbun, and Sheng Li. Learning infomax and domain-independent representations for causal effect inference with real-world data. In *Proceedings of the 2022 SIAM International Conference on Data Mining (SDM)*, pages 433–441. SIAM, 2022.
- [152] Liu Qidong, Tian Feng, Ji Weihua, and Zheng Qinghua. A new representation learning method for individual treatment effect estimation: Split covariate representation network. In *Asian Conference on Machine Learning*, pages 811–822. PMLR, 2020.
- [153] BN Prichard and PM Gillam. Assessment of propranolol in angina pectoris. clinical dose response curve and effect on electrocardiogram at rest and on exercise. *British heart journal*, 33(4):473, 1971.
- [154] ARTHUR B Schneider, ELAINE Ron, Jay Lubin, Marilyn Stovall, and Theresa C Gierlowski. Dose-response relationships for radiation-induced thyroid cancer and thyroid nodules: evidence for the prolonged effects of radiation on the thyroid. *The Journal of Clinical Endocrinology & Metabolism*, 77(2):362–369, 1993.
- [155] Timothy J Threlfall and Dallas R English. Sun exposure and pterygium of the eye: a dose-response curve. *American journal of ophthalmology*, 128(3):280–287, 1999.

- [156] Hao Zou, Bo Li, Jiangang Han, Shuiping Chen, Xuetao Ding, and Peng Cui. Counterfactual prediction for outcome-oriented treatments. In *International Conference on Machine Learning*, pages 27693–27706. PMLR, 2022.
- [157] Jennifer L Hill. Bayesian nonparametric modeling for causal inference. *Journal of Computational and Graphical Statistics*, 20(1):217–240, 2011.
- [158] Douglas Almond, Kenneth Y Chay, and David S Lee. The costs of low birth weight. *The Quarterly Journal of Economics*, 120(3):1031–1083, 2005.
- [159] Vincent Dorie, Jennifer Hill, Uri Shalit, Marc Scott, and Dan Cervone. Automated versus do-it-yourself methods for causal inference: Lessons learned from a data analysis competition. *Statistical Science*, 34(1):43–68, 2019.
- [160] Peter M Robinson. Root-n-consistent semiparametric regression. *Econometrica: Journal of the Econometric Society*, pages 931–954, 1988.
- [161] Yishai Shimoni, Chen Yanover, Ehud Karavani, and Yaara Goldschmidt. Benchmarking framework for performance-evaluation of causal inference analysis. *arXiv preprint arXiv:1802.05046*, 2018.
- [162] Marian F MacDorman and Jonnae O Atkinson. Infant mortality statistics from the linked birth/infant death data set–1995 period data. 1998.
- [163] Changran Geng, Harald Paganetti, and Clemens Grassberger. Prediction of treatment response for combined chemo-and radiation therapy for non-small cell lung cancer patients using a bio-mathematical model. *Scientific reports*, 7(1):1–12, 2017.
- [164] Dominique Barbolosi and Athanassios Iliadis. Optimizing drug regimens in cancer chemotherapy: a simulation study using a pk–pd model. *Computers in Biology and Medicine*, 31(3):157–172, 2001.
- [165] Miro J Eigenmann, Nicolas Frances, Thierry Lavé, and Antje-Christine Walz. Pkpd modeling of acquired resistance to anti-cancer drug treatment. *Journal of pharmacokinetics and pharmacodynamics*, 44(6):617–630, 2017.
- [166] Alistair EW Johnson, Tom J Pollard, Lu Shen, Li-wei H Lehman, Mengling Feng, Mohammad Ghassemi, Benjamin Moody, Peter Szolovits, Leo Anthony Celi, and Roger G Mark. Mimic-iii, a freely accessible critical care database. *Scientific data*, 3(1):1–9, 2016.
- [167] Mohammed Saeed, Mauricio Villarroel, Andrew T Reisner, Gari Clifford, Li-Wei Lehman, George Moody, Thomas Heldt, Tin H Kyaw, Benjamin Moody, and Roger G Mark. Multiparameter intelligent monitoring in intensive care ii (mimic-ii): a public-access intensive care unit database. *Critical care medicine*, 39(5):952, 2011.
- [168] Yue He, Zheyang Shen, and Peng Cui. Towards non-iid image classification: A dataset and baselines. *Pattern Recognition*, 110:107383, 2021.
- [169] Han Xiao, Kashif Rasul, and Roland Vollgraf. Fashion-mnist: a novel image dataset for benchmarking machine learning algorithms. *arXiv preprint arXiv:1708.07747*, 2017.
- [170] Clifford R Jack Jr, Matt A Bernstein, Nick C Fox, Paul Thompson, Gene Alexander, Danielle Harvey, Bret Borowski, Paula J Britson, Jennifer L. Whitwell, Chadwick Ward, et al. The alzheimer’s disease neuroimaging initiative (adni): Mri methods. *Journal of Magnetic Resonance Imaging: An Official Journal of the International Society for Magnetic Resonance in Medicine*, 27(4):685–691, 2008.
- [171] Christian Humpel and Tanja Hochstrasser. Cerebrospinal fluid and blood biomarkers in alzheimer’s disease. *World journal of psychiatry*, 1(1):8, 2011.
- [172] Chintan Ramani, Eric M Davis, John S Kim, J Javier Provencio, Kyle B Enfield, and Alex Kadl. Post-icu covid-19 outcomes: a case series. *Chest*, 159(1):215–218, 2021.
- [173] Emily Herrett, Arlene M Gallagher, Krishnan Bhaskaran, Harriet Forbes, Rohini Mathur, Tjeerd Van Staa, and Liam Smeeth. Data resource profile: clinical practice research datalink (cprd). *International journal of epidemiology*, 44(3):827–836, 2015.
- [174] Halil Bisgin, Nitin Agarwal, and Xiaowei Xu. Does similarity breed connection?-an investigation in blogcatalog and last. fm communities. In *2010 IEEE Second International Conference on Social Computing*, pages 570–575. IEEE, 2010.
- [175] Michael Stephens. Flickr. *Library Technology Reports*, 42(4):58–62, 2008.
- [176] Kwonsang Lee, Falco J Bargagli-Stoffi, and Francesca Dominici. Causal rule ensemble: Interpretable inference of heterogeneous treatment effects. *arXiv preprint arXiv:2009.09036*, 2020.
- [177] Falco J Bargagli-Stoffi, Kristof De-Witte, and Giorgio Gnecco. Heterogeneous causal effects with imperfect compliance: a novel bayesian machine learning approach. *arXiv preprint arXiv:1905.12707*, 2019.

- [178] Kosuke Imai and Michael Lingzhi Li. Experimental evaluation of individualized treatment rules. *Journal of the American Statistical Association*, pages 1–15, 2021.
- [179] Alicia Curth, David Svensson, Jim Weatherall, and Mihaela van der Schaar. Really doing great at estimating cate? a critical look at ml benchmarking practices in treatment effect estimation. In *Thirty-fifth Conference on Neural Information Processing Systems Datasets and Benchmarks Track (Round 2)*, 2021.
- [180] David Jensen. Comment: Strengthening empirical evaluation of causal inference methods. *Statistical Science*, 34(1):77–81, 2019.
- [181] Lu Cheng, Ruocheng Guo, Raha Moraffah, K Selçuk Candan, Adrienne Raglin, and Huan Liu. A practical data repository for causal learning with big data. In *International Symposium on Benchmarking, Measuring and Optimization*, pages 234–248. Springer, 2019.
- [182] P Richard Hahn, Jared S Murray, and Carlos M Carvalho. Bayesian regression tree models for causal inference: Regularization, confounding, and heterogeneous effects (with discussion). *Bayesian Analysis*, 15(3):965–1056, 2020.
- [183] Jean Kaddour, Yuchen Zhu, Qi Liu, Matt J Kusner, and Ricardo Silva. Causal effect inference for structured treatments. *Advances in Neural Information Processing Systems*, 34:24841–24854, 2021.
- [184] Jonathan D Young, Bryan Andrews, Gregory F Cooper, and Xinghua Lu. Learning latent causal structures with a redundant input neural network. In *Proceedings of the 2020 KDD Workshop on Causal Discovery*, pages 62–91. PMLR, 2020.
- [185] Junpeng Zhang, Vu Viet Hoang Pham, Lin Liu, Taosheng Xu, Buu Truong, Jiuyong Li, Nini Rao, and Thuc Duy Le. Identifying mirna synergism using multiple-intervention causal inference. *BMC bioinformatics*, 20(23):1–11, 2019.
- [186] Christopher Schmidt, Johannes Huegle, Siegfried Horschig, and Matthias Uflacker. Out-of-core gpu-accelerated causal structure learning. In *International Conference on Algorithms and Architectures for Parallel Processing*, pages 89–104. Springer, 2019.
- [187] Jonathan Young. *Deep Learning for Causal Structure Learning Applied to Cancer Pathway Discovery*. PhD thesis, University of Pittsburgh, 2020.
- [188] Cheng-Ying Chou, Wan-I Chang, Tzyy-Leng Horng, and Win-Li Lin. Numerical modeling of nanodrug distribution in tumors with heterogeneous vasculature. *PLoS One*, 12(12):e0189802, 2017.
- [189] Ruibo Tu, Kun Zhang, Bo Bertilson, Hedvig Kjellstrom, and Cheng Zhang. Neuropathic pain diagnosis simulator for causal discovery algorithm evaluation. *Advances in Neural Information Processing Systems*, 32, 2019.
- [190] Spyridon Patmanidis, Alexandros C Charalampidis, Ioannis Kordonis, Katerina Strati, Georgios D Mitsis, and George P Papavassilopoulos. Individualized growth prediction of mice skin tumors with maximum likelihood estimators. *Computer Methods and Programs in Biomedicine*, 185:105165, 2020.
- [191] Ioana Bica, Ahmed M Alaa, Craig Lambert, and Mihaela Van Der Schaar. From real-world patient data to individualized treatment effects using machine learning: current and future methods to address underlying challenges. *Clinical Pharmacology & Therapeutics*, 109(1):87–100, 2021.
- [192] Kaouter Karboub and Mohamed Tabaa. A machine learning based discharge prediction of cardiovascular diseases patients in intensive care units. In *Healthcare*, volume 10, page 966. Multidisciplinary Digital Publishing Institute, 2022.
- [193] Chang Liu, Xinwei Sun, Jindong Wang, Haoyue Tang, Tao Li, Tao Qin, Wei Chen, and Tie-Yan Liu. Learning causal semantic representation for out-of-distribution prediction. *Advances in Neural Information Processing Systems*, 34:6155–6170, 2021.
- [194] Xinwei Sun, Botong Wu, Xiangyu Zheng, Chang Liu, Wei Chen, Tao Qin, and Tie-Yan Liu. Recovering latent causal factor for generalization to distributional shifts. *Advances in Neural Information Processing Systems*, 34:16846–16859, 2021.
- [195] Tan Wang, Chang Zhou, Qianru Sun, and Hanwang Zhang. Causal attention for unbiased visual recognition. In *Proceedings of the IEEE/CVF International Conference on Computer Vision*, pages 3091–3100, 2021.
- [196] Zhaoquan Yuan, Xiao Peng, Xiao Wu, Bing-kun Bao, and Changsheng Xu. Meta-learning causal feature selection for stable prediction. In *2021 IEEE International Conference on Multimedia and Expo (ICME)*, pages 1–6. IEEE, 2021.
- [197] Yuqing Wang, Xiangxian Li, Zhuang Qi, Jingyu Li, Xuelong Li, Xiangxu Meng, and Lei Meng. Meta-causal feature learning for out-of-distribution generalization. *arXiv preprint arXiv:2208.10156*, 2022.

- [198] Pramuditha Perera, Ramesh Nallapati, and Bing Xiang. Ocgan: One-class novelty detection using gans with constrained latent representations. In *Proceedings of the IEEE/CVF Conference on Computer Vision and Pattern Recognition*, pages 2898–2906, 2019.
- [199] Matthew O’Shaughnessy, Gregory Canal, Marissa Connor, Christopher Rozell, and Mark Davenport. Generative causal explanations of black-box classifiers. *Advances in Neural Information Processing Systems*, 33:5453–5467, 2020.
- [200] Chao-Han Huck Yang, Yi-Chieh Liu, Pin-Yu Chen, Xiaoli Ma, and Yi-Chang James Tsai. When causal intervention meets adversarial examples and image masking for deep neural networks. In *2019 IEEE International Conference on Image Processing (ICIP)*, pages 3811–3815. IEEE, 2019.
- [201] Yu Yao, Tongliang Liu, Mingming Gong, Bo Han, Gang Niu, and Kun Zhang. Instance-dependent label-noise learning under a structural causal model. *Advances in Neural Information Processing Systems*, 34:4409–4420, 2021.
- [202] Thien Q Tran, Kazuto Fukuchi, Youhei Akimoto, and Jun Sakuma. Unsupervised causal binary concepts discovery with vae for black-box model explanation. In *Proceedings of the AAAI Conference on Artificial Intelligence*, volume 36, pages 9614–9622, 2022.
- [203] Andrew Jesson, Sören Mindermann, Uri Shalit, and Yarin Gal. Identifying causal-effect inference failure with uncertainty-aware models. *Advances in Neural Information Processing Systems*, 33:11637–11649, 2020.
- [204] Shruti Tople, Amit Sharma, and Aditya Nori. Alleviating privacy attacks via causal learning. In *International Conference on Machine Learning*, pages 9537–9547. PMLR, 2020.
- [205] Sebastian Pölsterl and Christian Wachinger. Estimation of causal effects in the presence of unobserved confounding in the alzheimer’s continuum. In *International Conference on Information Processing in Medical Imaging*, pages 45–57. Springer, 2021.
- [206] Baoliang Zhang, Xiaoxin Guo, Qifeng Lin, Haoren Wang, and Songbai Xu. Counterfactual inference graph network for disease prediction. *Knowledge-Based Systems*, page 109722, 2022.
- [207] Christian Wachinger, Benjamin Gutierrez Becker, Anna Rieckmann, and Sebastian Pölsterl. Quantifying confounding bias in neuroimaging datasets with causal inference. In *International Conference on Medical Image Computing and Computer-Assisted Intervention*, pages 484–492. Springer, 2019.
- [208] Rongguang Wang, Pratik Chaudhari, and Christos Davatzikos. Harmonization with flow-based causal inference. In *International Conference on Medical Image Computing and Computer-Assisted Intervention*, pages 181–190. Springer, 2021.
- [209] Nina Van Goethem, Ben Serrien, Mathil Vandromme, Chloé Wyndham-Thomas, Lucy Catteau, Ruben Brondeel, Sofieke Klammer, Marjan Meurisse, Lize Cuypers, Emmanuel André, et al. Conceptual causal framework to assess the effect of sars-cov-2 variants on covid-19 disease severity among hospitalized patients. *Archives of Public Health*, 79(1):1–12, 2021.
- [210] Harrison Wilde, Thomas Mellan, Iwona Hawryluk, John M Dennis, Spiros Denaxas, Christina Pagel, Andrew Duncan, Samir Bhatt, Seth Flaxman, Bilal A Mateen, et al. The association between mechanical ventilator compatible bed occupancy and mortality risk in intensive care patients with covid-19: a national retrospective cohort study. *BMC medicine*, 19(1):1–12, 2021.
- [211] Atalanti Mastakouri and Bernhard Schölkopf. Causal analysis of covid-19 spread in germany. *Advances in Neural Information Processing Systems*, 33:3153–3163, 2020.
- [212] Emilia Gvozdenović, Lucio Malvisi, Elisa Cinconze, Stijn Vansteelandt, Phoebe Nakanwagi, Emmanuel Aris, and Dominique Rosillon. Causal inference concepts applied to three observational studies in the context of vaccine development: from theory to practice. *BMC medical research methodology*, 21(1):1–10, 2021.
- [213] Marie-Laure Charpignon, Bella Vakulenko-Lagun, Bang Zheng, Colin Magdamo, Bowen Su, Kyle Evans, Steve Rodriguez, Artem Sokolov, Sarah Boswell, Yi-Han Sheu, et al. Drug repurposing of metformin for alzheimer’s disease: Combining causal inference in medical records data and systems pharmacology for biomarker identification. *medRxiv*, 2021.
- [214] Shishir Rao, Mohammad Mamouei, Gholamreza Salimi-Khorshidi, Yikuan Li, Rema Ramakrishnan, Abdelaali Hassaine, Dexter Canoy, and Kazem Rahimi. Targeted-behrt: Deep learning for observational causal inference on longitudinal electronic health records. *arXiv preprint arXiv:2202.03487*, 2022.
- [215] Jie Zhu and Blanca Gallego. Cds—causal inference with deep survival model and time-varying covariates. *arXiv preprint arXiv:2101.10643*, 2021.

- [216] Janie Coulombe. *Causal Inference on the Marginal Effect of an Exposure: Addressing Biases Due to Covariate-Driven Monitoring Times and Confounders*. PhD thesis, McGill University (Canada), 2021.
- [217] Antonia Marsden. *Causal Modelling in Stratified and Personalised Health: Developing Methodology for Analysis of Primary Care Databases in Stratified Medicine*. The University of Manchester (United Kingdom), 2016.
- [218] Jundong Li, Ruocheng Guo, Chenghao Liu, and Huan Liu. Adaptive unsupervised feature selection on attributed networks. In *Proceedings of the 25th ACM SIGKDD International Conference on Knowledge Discovery & Data Mining*, pages 92–100, 2019.
- [219] Jundong Li, Xia Hu, Jiliang Tang, and Huan Liu. Unsupervised streaming feature selection in social media. In *Proceedings of the 24th ACM International on Conference on Information and Knowledge Management*, pages 1041–1050, 2015.
- [220] Vincent Dorie. Npci: Non-parametrics for causal inference. URL: <https://github.com/vdorie/npci>, 2016.
- [221] Rajeev H Dehejia and Sadek Wahba. Propensity score-matching methods for nonexperimental causal studies. *Review of Economics and statistics*, 84(1):151–161, 2002.
- [222] Jeffrey A Smith and Petra E Todd. Does matching overcome lalonde’s critique of nonexperimental estimators? *Journal of econometrics*, 125(1-2):305–353, 2005.